Energy Circuit Security Region of Energy System (I): Concepts and Models

Jun Xiao, *Member*, *IEEE*, Cong Wang, Chenhui Song, *Member*, *IEEE*, Xun Jiang, *Member*, *IEEE*
Chengjin Li, and Gang Sun

***Abstract*—The security region defines the maximum allowable operating range of a system, which has been developed as an important tool for security analysis of energy systems. However, due to distinct physical transport processes and mathematical representations associated with heterogeneous energy sources, there is currently no unified standardized models for security regions, which makes the security region model of integrated energy system (IES) even more intricate. In this regard, we propose the energy circuit security region (ECSR), which achieves a unified modeling and solution framework for the security regions of electrical power system (EPS), natural gas system (NGS) and integrated energy system. This paper, as the preliminary work on the ECSR, focuses on the development of concepts and models. Firstly, the concepts and models of security region for IES are presented. Secondly, the models of energy circuit for unified modeling of heterogeneous energy sources are introduced: the energy circuit is represented as the electrical circuit in EPS and the gas circuit in NGS; we derive the gas circuit model by analogy with the electrical circuit model. Thirdly, the models about ECSR of energy systems are proposed, which are very concise when representing the security region of IES and can be simplified into the security regions of EPS and NGS. Finally, the developed model is verified by using typical cases of EPS, NGS and IES. The results show that the proposed method achieves the unity of the mathematical models of the security region among a single heterogeneous energy system and IES, which makes it feasible to apply mature security analysis methods of EPS to other non-EPSs and develop more in-depth observational analysis methods for cross-heterogeneous energy subsystems.**

***Index Terms*—integrated energy system; electrical power s ystem; natural gas system; security region; energy circuit**

I. Introduction

INTEGRATED Energy System (IES) is designed around heterogeneous energy sources like electricity and natural gas, facilitating synergistic complementarity and cascaded energy utilization through multi-energy coupling. It serves as a pivotal platform for establishing the Energy Internet. Nevertheless, multi-energy coupling escalates the security risks associated with system operation [2]. Disturbances, as they propagate across different energy systems, can readily trigger more extensive cascading failures [2-3]. Notable examples include the "8.9" blackout in the UK, the "8.14" blackout in California, and the February power outage in Texas, USA. This underscores the necessity, in the context of IES, to not only ensure the safe operation of individual energy systems but also to address the security concerns arising from system interactions. A comprehensive analysis of IES security from an integrated perspective is therefore warranted [4].

The exploration of IES security remains in its preliminary stages, predominantly revolving around the "point-by-point method" [2,4]. However, this approach is beset with certain limitations [5]: (1) Each instance of security verification necessitates the pre-execution of multiple energy flow calculations, a time-intensive process that falls short of meeting the real-time requisites of security analysis; (2) It fails to encompass a comprehensive depiction of the complete operational range and security boundaries of the IES, thereby failing to provide holistic metrics of operating point security, adaptable margins, and other pertinent insights sought after by dispatchers and stakeholders within the market.

In comparison to the "point-by-point method," the security region approach presents distinct advantages [6]: (1) By relocating energy flow calculations and related processes to offline preparation, it substantially enhances the real-time efficiency of security analysis; (2) Calculation of the distance from the operating point to the security boundary yields a quantification of the security margin; (3) Comprehensive system-wide security information can be derived, enabling enhanced situational awareness and proactive preventive measures. As a result, researchers have drawn inspiration from the security region the electric power system (EPS-SR) and extended their investigations to the security region concept within the integrated energy system (IES-SR) [5,7-13]. The inception of the IES-SR concept and model can be traced back to the seminal work in Ref. [7]. Subsequent research endeavors [5,8-13] have further advanced upon the foundation laid by Ref. [7]. Ref. [8] addresses the stochastic nature of wind power and introduces a robust IES-SR framework based on convex hulls. Ref. [5] delves into N-1 security considerations. Ref. [9] undertakes a thorough examination of the security region

Received xxxxxxxxx; revised xxxxxxxxxx; accepted xxxx. Date of publication xxxxxxxxxxxx; date of current version xxxxxxxxxxxxxx. This work was supported in part by the National Natural Science Foundation of China under Grant 52307079 and in part by the Natural Science Foundation of Hunan Province under Grant 2024JJ6050. *(Corresponding author: Chenhui Song.)*

Jun Xiao, Cong Wang, Chengjin Li and Gang Sun are with the State Key Laboratory of Intelligent Power Distribution Equipment and System, Tianjin University, Tianjin 300072, China(e-mail: xiaojun@tju.edu.cn; 13082328819@163.com; lichengji@tju.edu.cn; sun_gang2000@163.com).

Chenhui Song is with the State Key Laboratory of Disaster Prevention & Reduction for Power Grid, Changsha University of Science and Technology, Changsha, China and also with the State Key Laboratory of Intelligent Power Distribution Equipment and System, Tianjin University, Tianjin 300072, China (e-mail:songchenhui66399@163.com).

Xun Jiang is with the School of Engineering, Cardiff University, Cardiff, CF24 3AA, the UK.(e-mail: jiangx28@cardiff.ac.uk).

pertaining to natural gas networks within IES. In the context of modeling IES-SR, Ref. [10] undertakes a comprehensive incorporation of multi-energy flow dynamics and pressure constraints inherent to heterogeneous energy sources. Ref. [11-12] undertake investigations into the topological attributes of IES-SR alongside a dynamic-based security region resolution method. Ref. [13] proposes an energy hub-centric security region to characterize IES load supply capabilities. Ref. [14] introduces a steady-state IES-SR model that takes thermal dynamics into account.

The security region approach indeed addresses the limitations of the "point-by-point method". However, the lack of standardized models that strike a balance between accuracy and complexity across diverse heterogeneous energy systems still poses a challenge. Consequently, the extensive array of mature methods in EPS often finds limited applicability when extended to the analysis of non-EPSs. Several pressing issues remain to be addressed: Existing steady-state models of IES-SR predominantly derive from the intrinsic energy flow equations characterizing heterogeneous energy systems, which predominantly manifest as nonlinear relationships. The diverse array of mathematical forms and solution methodologies [15] accentuate the intricacy associated with solving IES-SR, particularly in the context of high-dimensional IES-SR problems. Although no specific offline time frame is stipulated for security region computation, the exhaustive calculation of high-dimensional security region outcomes for large scale IESs might impose substantial demands on computational resources and time. If not meticulously managed for computational efficiency, this could lead to substantial time and resource consumption during offline computations, thereby hampering the prompt derivation of computation outcomes.

The solution to the aforementioned challenge is found in the unified modeling approach for heterogeneous energy [16-28]. This method hinges on considering dissimilar transmission traits of heterogeneous energy alongside the semblance of network features, leading to the establishment of a harmonized mathematical framework under specific conditions [16]. Typically, this assumes the form of algebraic equations constituting standardized network equations. Furthermore, this unified modeling technique for heterogeneous energy employs equivalent parameters for facilitating information exchange among diverse systems. This circumvents the necessity for direct disclosure of actual pipeline network parameters, a measure that enhances data privacy safeguards and mitigates information barriers in the operational realm of actual heterogeneous energy systems. Unified modeling methods encompass primarily the energy circuit theory [16-22], generalized electric circuit theory [23-25], and various other equivalent modeling methods [26-28]. In this paper, our primary focus rests on the energy circuit theory [16-22]. The research of energy circuit mainly encompasses modeling methodologies [16,18-19], multi-energy flow calculations [16,20], state estimation [21], and optimized scheduling [17,22]. However, no research regarding on security region have been identified to date.

This paper develops the theory of energy circuit security region (ECSR) in energy systems. Serving as the preliminary work on the ECSR, this paper predominantly examines the concept and model. The subsequent content is organized as follows. The first section elaborates on the overarching concept and model of security region. The second section presents an energy circuit model for the unified modeling of heterogeneous energy systems, which includes the derivation of gas circuit models and network equations of NGS. The third section establishes security region models for energy systems encompassing EPS, NGS, and IES. The fourth section conducts cases verification of the method proposed in this paper, analyzing the strengths through comparison with existing methods. In addition, the Nomenclature section is shown in Appendix A.

II. Concepts and Models of Security Region

A. Operating point

The power system employs operating points for security delineation [6]. Referring to the power system, we define a universal concept for operating points within the energy systems: the minimum set of variables that can describe the security of the system's operating state. In the forthcoming energy system, the load represents the demand-side entity, while power supply, gas sources and others constitute the supply-side service entities. These service entities are tasked with aiding the system in fulfilling its security operational requisites per the agreement [1]. Consequently, the operating point variables for each energy system can be uniformly selected as node loads:

$$\boldsymbol{W} = [S_{\mathrm{l,e1}},...,S_{\mathrm{l},ei},...,S_{\mathrm{l},em},G_{\mathrm{l,g1}},...,G_{\mathrm{l,g}\,j},...,G_{\mathrm{l,g}\,n}] \tag{1}$$

where, $\boldsymbol{W}$ represents the operating point; $S_{\mathrm{l},ei}$ is the power of power load node i; $G_{\mathrm{l},gj}$ is the flow rate of natural gas load node j; i=0,1,2,...,m, m is the number of power load nodes; j=0,1,2,...,n, n is the number of natural gas load nodes.

Diverging from single-energy systems, IES forges interconnections between heterogeneous energy systems through coupling units. In this paper, two emblematic coupling units are featured, as illustrated in Figure 1: natural gas compressors as the electric loads, driving power from the electrical system; while gas generators operate as natural gas loads, receiving input from the natural gas system.

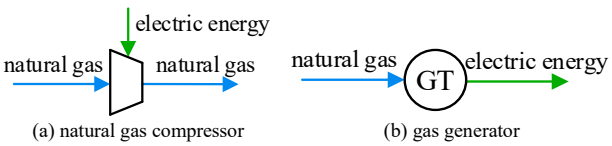

Fig. 1. Schematic diagram of typical coupling units.

For IES, in order to differentiate between the load of the coupling unit and the intrinsic load of each heterogeneous energy system, this paper article expresses the operating point in the form of equation (2).

$$\boldsymbol{W} = [S_{\mathrm{l,e1}},...,S_{\mathrm{l},ei},...,S_{\mathrm{l,c1}},...,S_{\mathrm{l},cm},...G_{\mathrm{l,g1}},\\ ...,G_{\mathrm{l,g}\,j},...,G_{\mathrm{l,GT1}},...,G_{\mathrm{l,GT}n},...] \tag{2}$$

where, $S_{\mathrm{l},cm}$ is the electric energy required to drive compressor m; $G_{\mathrm{l,GT}n}$ is the natural gas input by the gas generator n.

B. Security

Referring to the EPS, the general definition of security for energy system is as follows: for a given operational point, it's considered secure if all the operational constraints for the corresponding states are satisfied. The secure operational point is denoted as "$\boldsymbol{W}_{\mathrm{s}}$". Conversely, if any constraint is not met, it indicates a risk in the system operation, which makes the point insecure.

It's important to clarify: (1) While the security region employs the operating point (node power/gas flow) as a variable, other state variables such as node voltage/pressure, branch power, pipeline flow, etc., are also interconnected with the operating point. An operating point is deemed secure only when all state variables conform to the security constraints, which can be divided into two situations: if the current state is secure, the control variables do not need to be adjusted, the system is judged secure; if the current state is insecure, the control variables shall be adjusted, if it can make the system secure after adjustment, the operating point is a secure point, otherwise, the operating point should be judged as insecure. (2) The definition of security above draws inspiration from the secure operation of the power system, known as N-0 security [29]. "Insecure" indicates that the operating point is not within a "secure" state, it doesn't necessarily imply an immediate failure. "Insecure" can introduce latent risks. If operations persist with latent risks, it may eventually lead to failures.

C. Security region

In reference to the EPS, the security region of the energy system is defined as the ensemble of all secure operating points arising during system operation [6], represented as $\boldsymbol{\Omega}_{\mathrm{SR}}$. The mathematical model is articulated as follows.

$$\boldsymbol{\Omega}_{\mathrm{SR}} = \left\{ \boldsymbol{W}_{\mathrm{s}} \middle| \boldsymbol{h}(\boldsymbol{W}_{\mathrm{s}}) = \boldsymbol{0},\ \boldsymbol{g}(\boldsymbol{W}_{\mathrm{s}}) \le \boldsymbol{0} \right\} \tag{3}$$

where, $\boldsymbol{\Omega}_{\mathrm{SR}}$ is the universal symbol of security region for various systems, while $h(\boldsymbol{W}\mathrm{s})=0$ and $\mathrm{g}(\boldsymbol{W}\mathrm{s})\le 0$ respectively represent the equality and inequality constraints which need to be satisfied for the system to operate securely.

III. Energy Circuit based Unified Modeling Method of Heterogeneous Energy

A. Concept of unified modeling of heterogeneous energy

The unified modeling of heterogeneous energy [16-28] offers a solution to unify the security region of different energy systems. The concept revolves around recognizing the disparities in transmission characteristics among heterogeneous energy systems and the commonalities in network characteristics. It involves establishing a unified standardized model under specific conditions [16], typically in the form of algebraic equations and standardized network equations.

Energy circuit [16-22] and generalized electric circuit [23-25] are two widely employed models in the unified modeling of heterogeneous energy systems. Despite differences in assumptions, equivalence, transformations, and other specific details between the two, their fundamental concepts and implications are essentially identical, resulting in the same unified modeling outcome. Given that the nomenclature of "energy circuit" better encapsulates the equivalence relationship of heterogeneous energy within IES, this paper opts to utilize the energy circuit and its associated symbols for the unified modeling of the security region.

B. Energy circuit model

1) Electric circuit and network equations of EPS

The energy circuit model is depicted as the electric circuit within the EPS, typically employing the π-type electric circuit illustrated in Figure 2 to represent the energy circuit and equate power branches [16]. In Figure 2, Z_{eb} and $Y_{\mathrm{eb}0}$ denote the branch impedance and ground admittance of the line, while l_{e} indicates the length of the line. The corresponding network equation is as follows:

$$\boldsymbol{Y}_{\mathrm{e}}\boldsymbol{U}_{\mathrm{n}} = \boldsymbol{I}_{\mathrm{n}} \tag{4}$$

where, $\boldsymbol{Y}_{\mathrm{e}}$ is the matrix of node admittance; $\boldsymbol{U}_{\mathrm{n}}$ and $\boldsymbol{I}_{\mathrm{n}}$ are vectors composed of node voltage and injection current, respectively.

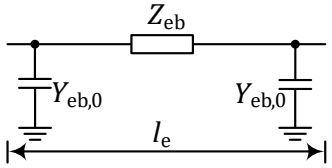

Fig. 2. Energy circuit of EPS: π-type electric circuit.

2) Gas circuit and network equations of NGS

The energy circuit model is represented as the gas circuit within the NGS [16,18], where pressure and natural gas flow correspond to the voltage and electric current in the electrical circuit. Given the fundamental nature of steady-state analysis, this paper conducts security region research based on steady-state models, with subsequent research addressing transient situations. Building upon the work in reference [18], this paper derives a steady-state gas circuit model for the NGS, encompassing the steady-state gas circuit and of pipeline and the network equation.

a. steady-state gas circuit of pipeline

By linearizing the momentum conservation equation of NGS and conducting circuit analogies, we can derive the energy circuit diagram of the NGS in the form of the gas circuit, as shown in Figure 3.

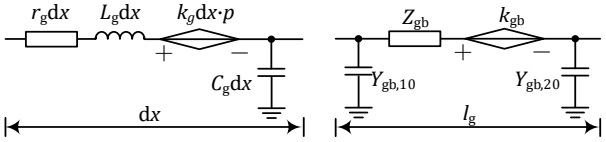

(a) gas circuit with distributed parameters (b) gas circuit with concentrated parameter

Fig. 3. Energy circuit of NGS: equivalent gas circuit

In Figure 3(a), we illustrate the gas circuit with distributed parameters, which represents the pressure drop and flow variations along a pipeline element with a length of dx. Figure 3(b) presents the equivalent π-shaped gas circuit with concentrated parameters [18]. For a detailed description of the modeling process, please refer to Appendix B.1.

In Figure 3(a), r_g, L_g, k_g, and C_g represent the distributed parameters of gas resistance, gas inductance, controlled gas pressure source, and gas capacitance, respectively. Under steady-state conditions, the treatment for "gas inductance as a short circuit and gas capacitance as an open circuit" leads to the following component equations:

$$r_g = \frac{\lambda_g v_b}{s_g d_g} \tag{5}$$

$$L_g = 0 \tag{6}$$

$$k_g = \frac{2gd_g \sin\theta_g - \lambda_g v_b^2}{2RTs_g} \tag{7}$$

$$C_g = 0 \tag{8}$$

where, λ_g, v_b, s_g, d_g, and θ_g represents the friction coefficient of the pipeline, the basic value of gas flow rate, cross-sectional area, inner diameter and inclination angle; g represents the acceleration of gravity; R and T represent the constant and temperature of natural gas. It should be noted that v_b is the main source of error in gas circuit modeling, its setting method is detailed in Appendix C.

In Figure 3(b), Z_{gb}, k_{gb}, $Y_{gb,10}$ and $Y_{gb,20}$ represent the branch impedance, controlled gas pressure source, and ground admittance in the form of concentrated parameters under the π-type gas circuit, with l_g representing the length of pipe. At steady state, the calculation equation for these parameters are as follows:

$$Z_{gb} = 2\frac{r_g}{k_g} \cdot \sinh\frac{k_g l_g}{2} \cdot e^{-\frac{k_g l_g}{2}} \tag{9}$$

$$k_{gb} = (\cosh\frac{k_g l_g}{2} - \sinh\frac{k_g l_g}{2}) e^{-\frac{k_g l_g}{2}} \tag{10}$$

$$Y_{gb,10} = 0 \tag{11}$$

$$Y_{gb,20} = 0 \tag{12}$$

b. steady-state network equation

The network equations of NGS and EPS have the same mathematical form, the modeling results at steady-state are shown in equation (13). The corresponding modeling process is detailed in Appendix B.2.

$$\boldsymbol{Y}_g \boldsymbol{p}_n = \boldsymbol{G}_n \tag{13}$$

where, $\boldsymbol{p}_n$ and $\boldsymbol{G}_n$ are vectors composed of node pressure and flow rate of natural gas, $\boldsymbol{Y}_g$ is the generalized node admittance matrix of NGS [16, 18]. The calculation equation is as follows:

$$\boldsymbol{Y}_g = -\boldsymbol{A}_g \boldsymbol{y}_{gb} (\boldsymbol{K}_g \boldsymbol{A}_{g+}^T - \boldsymbol{k}_{gb} \boldsymbol{A}_{g+}^T - \boldsymbol{A}_{g-}^T) \tag{14}$$

where, $\boldsymbol{A}_g$, $\boldsymbol{A}_{g+}$, $\boldsymbol{A}_{g-}$ are the node-branch incident matrix, node-outflow branch incident matrix, node-inflow branch incident matrix of NGS, their meanings are detailed in Appendix B.2. $\boldsymbol{K}_g$ is the matrix of compressor pressure ratio: for element $(\boldsymbol{K})_{i,i}$ in the i-th row and i-th column, use $(\boldsymbol{K})_{i,i}=K_g$ to indicate that branch i is connected to a compressor with a pressure ratio of K_g, otherwise take "1" as the value; $\boldsymbol{Y}_{gb}$ and $\boldsymbol{k}_{gb}$ are diagonal matrices composed of branch admittance and controlled gas pressure source of gas circuit in the π-type concentrated parameter, the matrix elements are the steady-state values of the concentrated parameter in the π-type gas circuit.

It should be noted that the natural gas flow rates in the above models are all based on mass flow rates. If using volumetric flow rate, it is necessary to convert it by dividing it by the natural gas density in the standard state after obtaining the final natural gas mass flow rate results.

3) Advantages of energy circuit model

Compared to the inherent energy balance equation of heterogeneous energy systems [10], the network equation of the energy path model has the following advantages:

(1) Better universality. Firstly, any energy system with a network structure can describe its energy balance relationship based on network equations. Secondly, network equations are the foundation of transient analysis, where partial differential equations are often transformed into algebraic network equations.

(2) Facilitate security analysis. On the one hand, network equations can be applied to security analysis, such as using the distribution coefficient method based on network equations to analyze the impact of branch interruptions in EPS; on the other hand, it is in line with the habits of security region research, such as using network equations for security region modeling in EPS [6].

IV. Energy Circuit Security Region Modeling

Energy circuit security region (ECSR) modeling refers to modeling the security region of an energy system based on the energy circuit. To verify the universality of the modeling method, first model the ECSR for a single energy system, then model the ECSR for the IES.

A. ECSR of EPS

Through using the network equation of EPS as a balance constraint for security region modeling, the following ECSR of EPS, represented as $\boldsymbol{\Omega}_{\text{EPS-ECSR}}$, can be obtained, which is as shown in equation (15).

$$\begin{cases} \boldsymbol{\Omega}_{\text{EPS-ECSR}} = \left\{ \boldsymbol{W}_s \middle| \boldsymbol{h}(\boldsymbol{W}_s) = \boldsymbol{0}, \boldsymbol{g}(\boldsymbol{W}_s) \le \boldsymbol{0} \right\} \\ s.t. \begin{cases} s.t.(15-1) \;\; \boldsymbol{Y}_e \boldsymbol{U}_n = \boldsymbol{I}_n \\ s.t.(15-2) \;\; \boldsymbol{I}_n^{\min} \le \boldsymbol{I}_n \le \boldsymbol{I}_n^{\max} \\ s.t.(15-3) \;\; \boldsymbol{U}_n^{\min} \le \boldsymbol{U}_n \le \boldsymbol{U}_n^{\max} \\ s.t.(15-4) \;\; \boldsymbol{I}_b \le \boldsymbol{I}_b^{\max} \\ s.t.(15-5) \;\; \boldsymbol{K}_e^{\min} \le \boldsymbol{K}_e \le \boldsymbol{K}_e^{\max} \end{cases} \end{cases} \tag{15}$$

The specific meanings of each constraint in equation (15) are as follows.

S.t. (15-1) is the constraint of network equation of EPS, where, $\boldsymbol{U}_n$ and $\boldsymbol{I}_n$ are vectors composed of node voltage and current, $\boldsymbol{Y}_e$ is the generalized node admittance matrix of EPS.

S.t. (15-2) is the constraint of upper and lower limits of node

current, where, $\boldsymbol{I}_{\mathrm{n}}^{\max}$ and $\boldsymbol{I}_{\mathrm{n}}^{\min}$ are vectors composed of the upper and lower limits of the node current.

S.t. (15-3) is the constraint of upper and lower limits of node voltage, where, $\boldsymbol{U}_{\mathrm{n}}^{\max}$ and $\boldsymbol{U}_{\mathrm{n}}^{\min}$ are vectors composed of the upper and lower limits of the node voltage.

S.t. (15-4) is the constraint of upper limit of the branch current, where, $\boldsymbol{I}_{\mathrm{b}}$ is the vector composed of the branch current, $\boldsymbol{I}_{\mathrm{b}}^{\max}$ is the vector composed of the current-carrying capacity.

S.t. (15-5) is the constraint of transformer ratio, where, $\boldsymbol{K}_{\mathrm{e}}$ is the transformer ratio matrix, $\boldsymbol{K}_{\mathrm{e}}^{\max}$ and $\boldsymbol{K}_{\mathrm{e}}^{\min}$ is the matrix formed by replacing the element of "$\boldsymbol{K}_{\mathrm{e}}$" with its upper and lower limit values.

B. ECSR of NGS

On the basis of the traditional model of NGS-SR, using network equation of NGS shown in equation (13) to replace the equation of pipeline pressure drop with gas flow [33], the ECSR of NGS, represented as $\boldsymbol{\Omega}_{\text{NGS-ECSR}}$, can be obtained, which is as shown in equation (16).

$$\begin{cases} \boldsymbol{\Omega}_{\text{NGS-ECSR}} = \left\{ \boldsymbol{W}_{\mathrm{s}} \middle| \boldsymbol{h}(\boldsymbol{W}_{\mathrm{s}}) = \boldsymbol{0}, \boldsymbol{g}(\boldsymbol{W}_{\mathrm{s}}) \le \boldsymbol{0} \right\} \\ s.t. \begin{cases} s.t.(16-1) \;\; \boldsymbol{Y}_{\mathrm{g}} \boldsymbol{p}_{\mathrm{n}} = \boldsymbol{G}_{\mathrm{n}} \\ s.t.(16-2) \;\; \boldsymbol{G}_{\mathrm{n}}^{\min} \le \boldsymbol{G}_{\mathrm{n}} \le \boldsymbol{G}_{\mathrm{n}}^{\max} \\ s.t.(16-3) \;\; \boldsymbol{p}_{\mathrm{n}}^{\min} \le \boldsymbol{p}_{\mathrm{n}} \le \boldsymbol{p}_{\mathrm{n}}^{\max} \\ s.t.(16-4) \;\; -\boldsymbol{A}_{\mathrm{g,L}}^{-1} \boldsymbol{G}_{\mathrm{n}} \le \boldsymbol{G}_{\mathrm{b}}^{\max} \\ s.t.(16-5) \;\; \boldsymbol{K}_{\mathrm{g}}^{\min} \le \boldsymbol{K}_{\mathrm{g}} \le \boldsymbol{K}_{\mathrm{g}}^{\max} \end{cases} \end{cases} \tag{16}$$

The specific meanings of each constraint are as follows.

S.t. (16-1) is the constraint of network equation of NGS, corresponding to the equation of pipeline pressure drop with gas flow in the traditional model of NGS-SR.

S.t. (16-2) is the constraint of upper and lower limits of node gas flow, where, $\boldsymbol{G}_{\mathrm{n}}^{\max}$ and $\boldsymbol{G}_{\mathrm{n}}^{\min}$ are the vectors composed of the upper and lower limits of the node gas flow.

S.t. (16-3) is the constraint of upper and lower limits of node gas pressure, where, $\boldsymbol{p}_{\mathrm{n}}^{\max}$ and $\boldsymbol{p}_{\mathrm{n}}^{\min}$ are vectors composed of the upper and lower limits of node pressure.

S.t. (16-4) is the upper limit constraint of pipeline gas flow, where, $\boldsymbol{A}_{\mathrm{g,L}}^{-1}$ is the left inverse matrix of the node-branch incident matrix $\boldsymbol{A}_{\mathrm{g}}$ of NGS; $\boldsymbol{G}_{\mathrm{b}}^{\max}$ is the vector of pipe capacity, which is composed of the upper limit of the gas flow allowed to be transported by the pipe.

S.t. (16-5) is the constraint of compressor pressure ratio, where, $\boldsymbol{K}_{\mathrm{g}}$ is the compressor pressure ratio matrix, $\boldsymbol{K}_{\mathrm{g}}^{\max}$ and $\boldsymbol{K}_{\mathrm{g}}^{\min}$ is the matrix formed by replacing the elements of "$\boldsymbol{K}_{\mathrm{g}}$" in the matrix with its upper and lower limit values.

C. ECSR of IES

By using the network equation as the balance constraint for IES-SR modeling, combined with the security constraints of IES operating and the constraints of coupling units, including the constraints of node voltage upper and lower limit, etc., the ECSR of IES, represented as $\boldsymbol{\Omega}_{\text{IES-ECSR}}$, can be obtained. Appendix D provides the detailed modeling process, the specific modeling result is shown in equation (17).

$$\begin{cases} \boldsymbol{\Omega}_{\text{IES-SR}} = \left\{ \boldsymbol{W}_{\mathrm{s}} \middle| \boldsymbol{h}(\boldsymbol{W}_{\mathrm{s}}) = \boldsymbol{0}, \boldsymbol{g}(\boldsymbol{W}_{\mathrm{s}}) \le \boldsymbol{0} \right\} \\ s.t.(17-1) \begin{cases} \boldsymbol{Y}_{\text{IES}} \boldsymbol{P}_{\mathrm{n}} = \boldsymbol{F}_{\mathrm{n}} \\ \boldsymbol{P}_{\mathrm{n}}^{\min} \le \boldsymbol{P}_{\mathrm{n}} \le \boldsymbol{P}_{\mathrm{n}}^{\max} \\ \boldsymbol{F}_{\mathrm{n}}^{\min} \le \boldsymbol{F}_{\mathrm{n}} \le \boldsymbol{F}_{\mathrm{n}}^{\max} \\ \boldsymbol{F}_{\mathrm{b}} \le \boldsymbol{F}_{\mathrm{b}}^{\max} \\ \boldsymbol{K}^{\min} \le \boldsymbol{K} \le \boldsymbol{K}^{\max} \end{cases} \\ s.t.(17-2) \begin{cases} \boldsymbol{g}_{\mathrm{m}} = f\left(\boldsymbol{h}_{\mathrm{m}}\right) \\ \boldsymbol{g}_{\mathrm{m}} \subseteq \boldsymbol{F}_{\mathrm{n}}, \boldsymbol{h}_{\mathrm{m}} \subseteq \boldsymbol{F}_{\mathrm{n}} \end{cases} \end{cases} \tag{17}$$

The specific meanings of each constraint in equation (17) are as follows.

S.t. (17-1) are the constraints of the IES network, including the network equation of IES, the constraint of upper and lower limits of node pressure, the constraint of upper and lower limits of node energy flow, the constraint of upper limit of branch energy flow, the generalized energy transformation ratio constraints formed by transformer transformation ratio constraints and compressor pressure ratio constraints. In *s.t.* (17-1), $\boldsymbol{Y}_{\text{IES}}$ is the generalized node admittance matrix of IES; $\boldsymbol{P}_{\mathrm{n}}$ and $\boldsymbol{F}_{\mathrm{n}}$ are vectors composed of node pressure (voltage or gas pressure) and energy flow (current or gas flow); $\boldsymbol{P}_{\mathrm{n}}^{\max}$ and $\boldsymbol{P}_{\mathrm{n}}^{\min}$ are vectors composed of the upper and lower limits of node pressure, respectively; $\boldsymbol{F}_{\mathrm{n}}^{\max}$ and $\boldsymbol{F}_{\mathrm{n}}^{\min}$ are vectors composed of the upper and lower limits of node flow; $\boldsymbol{F}_{\mathrm{b}}^{\max}$ is the upper limit of allowable transmission flow of the branch; $\boldsymbol{K}$ is the generalized energy transformation ratio matrix, composed of the transformation ratio matrix $\boldsymbol{K}_{\mathrm{e}}$ and the compressor pressure ratio matrix $\boldsymbol{K}_{\mathrm{g}}$. $\boldsymbol{K}^{\max}$ and $\boldsymbol{K}^{\min}$ are matrices formed by replacing the elements in $\boldsymbol{K}$ with their upper and lower limits.

S.t. (17-2) are the constraints for the operation of coupling units, expressed as a function of the output energy flow $\boldsymbol{g}_{\mathrm{m}}$ and input energy flow $\boldsymbol{h}_{\mathrm{m}}$ of the coupling unit, which describes the energy flow relationship of heterogeneous energy in IES. This paper selects electric driven compressors and gas generators as the coupling units, so the corresponding constraints include the equation for driving the power consumption of compressor and the equation for gas consumption of gas generator, as follows.

$$\begin{cases} S_{\mathrm{c}} = \dfrac{151.4653 \mathrm{p}_0 Z T G_c \kappa}{\psi \mathrm{T}_0 (\kappa\text{-}1)} \left(K_{\mathrm{g}}^{\frac{\kappa}{\kappa\text{-}1}} - 1 \right) \\ G_{\mathrm{GT}} = \dfrac{1}{\mathrm{V}_{\mathrm{GH}}} \left(a_{\mathrm{GT}} P_{GT}^2 + b_{\mathrm{GT}} P_{GT} + c_{\mathrm{GT}} + \left| d_{\mathrm{GT}} \sin\left(e_{\mathrm{GT}} \left(P_{\mathrm{GT}}^{\min} - P_{GT} \right) \right) \right| \right) \end{cases} \tag{18}$$

where, S_{c} is the power consumption for driving compressor; p_0 and T_0 are the standard atmospheric pressure and standard temperature; Z and κ are the compression factor and adiabatic constant of natural gas; ψ and K_{g} represent the efficiency and pressure ratio of the compressor; V_{GH} is the total calorific value of natural gas; G_{GT} is the gas consumption of the generator; a_{GT}, b_{GT}, c_{GT}, d_{GT}, e_{GT} are the heat consumption coefficients of gas

generator; P_{GT} is the active power output by the gas generator; P_{GT}^{min} is the lower limit of P_{GT}.

Comparing equations (15) to (17), it can be seen for the ECSR, whether it is for a single energy system or for the IES, the network equation, which is the first equation of constraints (15-1), (16-1) and (17-1), can be used to describe the energy balance relationship. Other constraints only need to consider the security of components.

V. Case Study

To verify the universality of modeling method of ECSR in this paper, two single energy systems of EPS and NGS, an IES coupled with electricity and gas, are selected as cases. To illustrate the process and results of modeling of ECSR, the original structure and component parameters of each energy system are provided firstly; then, diagrams of energy circuit are drawn based on the system structure; finally, modeling results of the ECSR are presented.

A. Case information

1) EPS

For EPS, IEEE 14-bus system is taken as the case to verify, as shown in Figure E1 of Appendix E, including buses N_{e1}~N_{e14}, branches b_{e1}~b_{e20}, transformers T_{e1}~T_{e3}. The detailed parameters are shown in Tables E1 and E2 of Appendix E.

2) NGS

For NGS, southeastern Belgium pipeline system is taken as the case to verify, as shown in E2 of Appendix E, including nodes N_{g1}~N_{g9}, pipes b_{g1}~b_{g11}, compressors C_{g1}~C_{g3}. The detailed parameters are shown in Tables E3~E5 of Appendix E.

3) IES

For IES, the 23-node system shown in Figure E3 of Appendix E is taken as the case to verify. The system is composed of southeastern Belgium pipeline system and IEEE 14-bus system. The electrical power required to drive compressors C_{g1}~C_{g3} is provided by buses N_{e13}, N_{e5} and N_{e4}; the natural gas required for gas generators G_{T1} and G_{T2} is provided by nodes N_{g5} and N_{g8}. The parameters are shown in Tables E6~E7 of Appendix E.

B. Diagrams of energy circuit

1) EPS

Based on the method in section 3.2.1 and the parameters in section 5.1.1, the IEEE14-bus system shown in Figure E1 can be equivalent to a diagram of energy circuit, as shown in the following Figure 4. The equivalent parts are marked in blue, including the distributed parameters of branches b_{e1}~b_{e20}, which are equivalent to the branch impedance and ground admittance in the form of concentrated parameters.

The diagram of energy circuit shown in Figure 4 is π-type equivalent circuit, which is commonly used in electrical network analysis.

2) NGS

Based on the method in section 3.2.2 and parameters in section 5.1.2, the southeastern Belgium pipeline system shown in Figure E2 can be equivalent to a diagram of energy circuit, as shown in Figure 5. The equivalent parts are marked in blue in the figure, including the original pipeline parameters of branches b_{g1}~b_{g11}, which are equivalent to the branch impedance and controlled gas pressure source in the form of concentrated parameters of gas circuit. The compressors in branches b_{e1}~b_{e2} and b_{g9} will be equivalent to transformers.

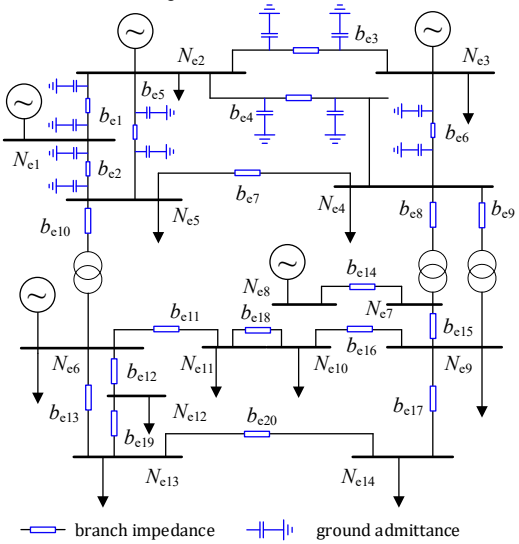

Fig. 4. Diagram of energy circuit of IEEE 14-bus system

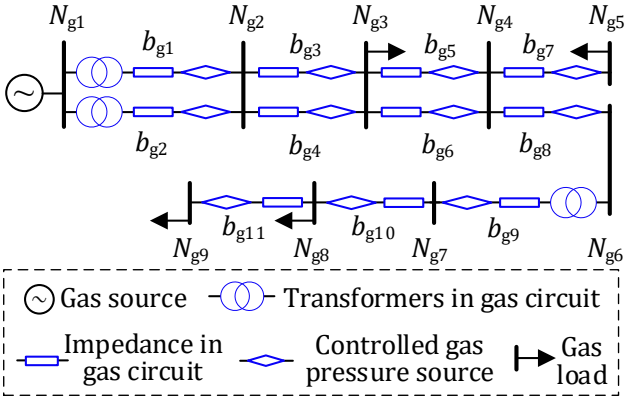

Fig. 5. Diagram of energy circuit of Belgium pipeline system

The diagram of energy circuit shown in Figure 5 is the equivalent gas circuit established by analogy with the equivalent electric circuit. The existing methods for natural gas network analysis do not establish an equivalent gas circuit, which cannot form a unified steady-state or transient analysis method, and the transient analysis process is very complex. Using the equivalent gas circuit for NGS analysis has the following advantages.

(1) Strong interpretability. Gas circuit components can be analogized to circuit components, which have clear physical meanings.

(2) Good uniformity. Similar to electric circuits, the gas circuit establishes a linear relationship between natural gas flow and pressure, making the steady-state and transient analysis methods of the gas network, as well as the analysis methods of NGS and EPS, unified. It can lay the foundation for the unified analysis of heterogeneous energy systems.

(3) The calculation difficulty is low. Based on gas circuit, the modeling of natural gas transient processes can be simplified from partial differential equations to algebraic equations, while

steady-state model is the special case of transient model.

3) IES

Based on the structure shown in Figure E3, Coupling the equivalent circuit of Figure 5 with the equivalent gas circuit of Figure 6, 23-node system of IES in Figure E3 will be equivalent to the diagram of energy circuit shown in Figure 6. According to the diagram of energy circuit, the network equation of IES can be directly established to describe the balance relationship of energy flow in the system.

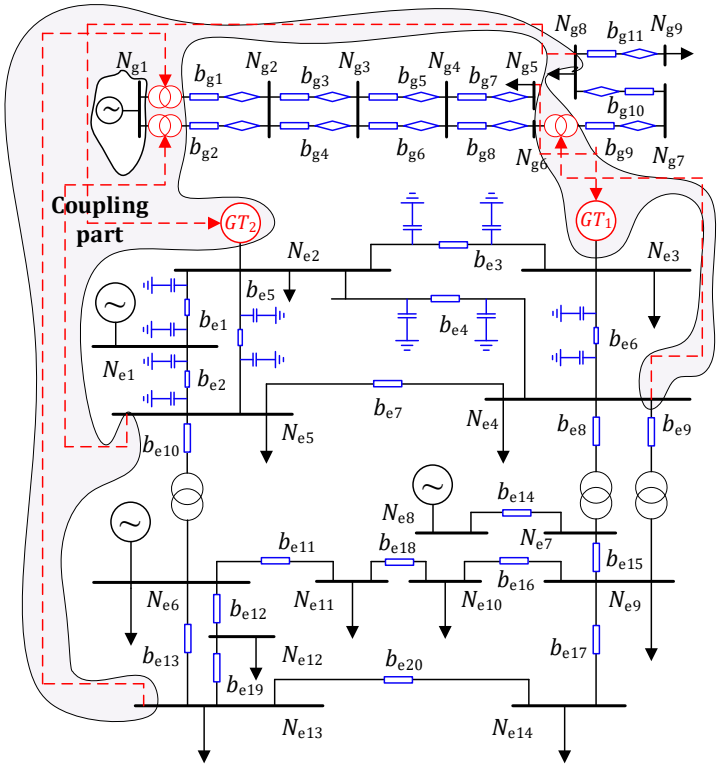

Fig. 6. Diagram of energy circuit of 23-node system of IES

C. Energy circuit security region

1) EPS

Firstly, calculate the circuit parameters, consider the branch characteristics and topology constraints, and represent the electric network equation according to equation (15-1) in section 3.2.1. Secondly, security constraints are represented based on the upper and lower limits of the operating range of components. Finally, based on the electric network equation and security constraints, ECSR of the IEEE 14-bus system can be obtained, as shown in the following equation (19).

2) NGS

Firstly, calculate the gas circuit parameters based on equations (5)~(8) in section 3.2.2. Secondly, considering the branch characteristics and topological constraints, the natural gas network equation can be represented according to equation (13) in section 3.2.2. Thirdly, security constraints are represented based on the upper and lower limits of the operating range of pipeline components. Finally, based on the natural gas network equation and security constraints, ECSR of the Belgium pipeline system can be obtained, as shown in the following equation (20).

3) IES

According to the derivation process and results in section 4.3, through substituting the parameters of EPS, NGS and coupling units into equation (18), IES-ECSR of the 23-node system can be obtained as the following equation (21)

$$
\begin{cases}
\boldsymbol{\Omega}_{\text{EPS-ECSR}}=\left\{\boldsymbol{W}_{\text{s}}=[S_{\text{l,e4}}\ S_{\text{l,e5}}\ S_{\text{l,e7}}\ S_{\text{l,e9}}\ S_{\text{l,e10}}\ S_{\text{l,e11}}\ S_{\text{l,e12}}\ S_{\text{l,e13}}\ S_{\text{l,e14}}]\,\middle|\,h(\boldsymbol{W}_{\text{s}})=0, g(\boldsymbol{W}_{\text{s}})\le 0\right\} \\
s.t.\begin{cases}
\boldsymbol{Y}_{\text{e}}\boldsymbol{U}_{\text{n}}=\boldsymbol{I}_{\text{n}} \\
[20\ 85\ 40\ 0\ 0\ 25\ 0\ 0\ 0\ 0\ 10]^{\text{T}}\le[S_{\text{l,e4}}\ S_{\text{l,e5}}\ S_{\text{l,e7}}\ S_{\text{l,e9}}\ S_{\text{l,e10}}\ S_{\text{l,e11}}\ S_{\text{l,e12}}\ S_{\text{l,e13}}\ S_{\text{l,e14}}]^{\text{T}} \\
\le[30\ 100\ 55\ 10\ 15\ 40\ 15\ 5\ 10\ 15\ 20]^{\text{T}} \\
[1.06\ 1.045\ 1.01\ 0.969\ 0.97\ 1.07\ 1.012\ 1.09\ 1.006\ 1.001\ 1.007\ 1.005\ 1\ 0.986]^{\text{T}}\le\boldsymbol{U}_{\text{n}} \\
\le[1.06\ 1.045\ 1.01\ 1.069\ 1.07\ 1.07\ 1.112\ 1.09\ 1.106\ 1.101\ 1.107\ 1.105\ 1\ 1.086]^{\text{T}} \\
[S_{\text{be1}}\ S_{\text{be2}}\ S_{\text{be3}}\ S_{\text{be4}}\ S_{\text{be5}}\ S_{\text{be6}}\ S_{\text{be7}}\ S_{\text{be8}}\ S_{\text{be9}}\ S_{\text{be10}}\ S_{\text{be11}}\ S_{\text{be12}}\ S_{\text{be13}}\ S_{\text{be14}}\ S_{\text{be15}}\ S_{\text{be16}}\ S_{\text{be17}}\ S_{\text{be18}}\ S_{\text{be19}}\ S_{\text{be20}}]^{\text{T}} \\
\le[200\ 100\ 100\ 75\ 50\ 50\ 75\ 50\ 25\ 75\ 25\ 25\ 25\ 25\ 50\ 10\ 25\ 10\ 5\ 10]^{\text{T}} \\
\boldsymbol{K}_{\text{e}}=[0.978\quad 0.969\quad 0.932]^{\text{T}}
\end{cases}
\end{cases}
\tag{19}
$$

$$\begin{cases} \boldsymbol{\Omega}_{\text{NGS-ECSR}}=\left\{\boldsymbol{W}_{\text{s}}=[G_{\text{l,e3}}\ G_{\text{l,e5}}\ G_{\text{l,e8}}\ G_{\text{l,e9}}]\middle| h(\boldsymbol{W}_{\text{s}})=0,\ g(\boldsymbol{W}_{\text{s}})\le 0\right\} \\ s.t.\begin{cases} \boldsymbol{Y}_{\text{g}}\boldsymbol{p}_{\text{n}}=\boldsymbol{G}_{\text{n}} \\ [69\ 126\ 0\ 0]^{\text{T}}\le[G_{\text{l,e3}}\ G_{\text{l,e5}}\ G_{\text{l,e8}}\ G_{\text{l,e9}}]^{\text{T}}\le[129\ 191\ 30\ 60]^{\text{T}} \\ [5.5\ 0\ 3\ 0\ 0\ 0\ 0\ 0\ 2.5]^{\text{T}}\le\boldsymbol{p}_{\text{n}}\le[6.5\ 6.5\ 6.5\ 6.5\ 6.5\ 6.5\ 6.3\ 6.5\ 6.5]^{\text{T}} \\ [G_{\text{bg1}}\ G_{\text{bg2}}\ G_{\text{bg3}}\ G_{\text{bg4}}\ G_{\text{bg5}}\ G_{\text{bg6}}\ G_{\text{bg7}}\ G_{\text{bg8}}\ G_{\text{bg9}}\ G_{\text{bg10}}\ G_{\text{bg11}}]^{\text{T}}\le[231.5\ 115.7\ 231.5\ 115.7\ 231.5\ 115.7\ 231.5\ 115.7\ 115.7\ 115.7\ 115.7]^{\text{T}} \\ [1\ 1\ 1]^{\text{T}}\le\boldsymbol{K}_{\text{g}}\le[1.2\ 1.2\ 1.2]^{\text{T}} \end{cases} \end{cases} \tag{20}$$

$$\begin{cases} \boldsymbol{\Omega}_{\text{IES-ECSR}}=\left\{\boldsymbol{W}_{\text{s}}=[S_{\text{l,e4}}\ S_{\text{l,e5}}\ S_{\text{l,e7}}\ S_{\text{l,e9}}\ S_{\text{l,e10}}\ S_{\text{l,e11}}\ S_{\text{l,e12}}\ S_{\text{l,e13}}\ S_{\text{l,e14}}\ G_{\text{l,e3}}\ G_{\text{l,e5}}\ G_{\text{l,e8}}\ G_{\text{l,e9}}]\middle| h(\boldsymbol{W}_{\text{s}})=0, g(\boldsymbol{W}_{\text{s}})\le 0\right\} \\ s.t.(22-1)\begin{cases} \boldsymbol{Y}_{\text{IES}}\boldsymbol{P}_{\text{n}}=\boldsymbol{F}_{\text{n}} \\ [1.06\ \ 1.045\ \cdots\ 0.986\ \ 5.5\ \ 0\ \cdots\ 2.5]\le[U_1\ \ U_2\ \cdots\ U_{14}\ \ p_1\ \ p_2\ \cdots\ p_9]\le[1.06\ \ 1.045\ \cdots\ 1.086\ \ 6.5\ \ 6.5\ \cdots\ 6.5] \\ [20\ \ 85\ \cdots\ 10\ \ 69\ \ 126\ \ 0\ \ 0]\le[S_{\text{l,e4}}\ \ S_{\text{l,e5}}\ \cdots\ S_{\text{l,e14}}\ \ G_{\text{l,e3}}\ \ G_{\text{l,e5}}\ \ G_{\text{l,e8}}\ \ G_{\text{l,e9}}]\le[30\ \ 100\ \cdots\ 20\ \ 129\ \ 191\ \ 30\ \ 60] \\ [S_{\text{be1}}\ \ S_{\text{be2}}\ \cdots\ S_{\text{be20}}\ \ G_{\text{bg1}}\ \ G_{\text{bg2}}\ \cdots\ G_{\text{bg11}}]\le[200\ 100\ \cdots\ 10\ 231.5\ 115.7\ \cdots\ 115.7] \\ [0.978\ \cdots\ 0.932\ \ 1\ \cdots\ 1]\le\boldsymbol{K}_{\text{IES}}\le[0.978\ \cdots\ 0.932\ \ 1.2\ \cdots\ 1.2] \end{cases} \\ s.t.(22-2)\begin{cases} S_{\text{c}}=\dfrac{151.4653p_0ZTG_c\kappa}{\psi T_0(\kappa\text{-}1)}(K_{\text{g}}^{\frac{\kappa}{\kappa\text{-}1}}-1) \\ G_{\text{GT}}=\dfrac{1}{\text{V}_{\text{GH}}}(0.01P_{GT}^2+4P_{GT}+150+|15\sin(0.5(P_{\text{GT}}^{\min}-P_{GT}))|) \end{cases} \end{cases} \tag{21}$$

4) Comparison with existing methods

Ref. [7] first proposed the concept and model of security region for IES. The subsequent related research [5, 8-12] extended the IES-SR based on Ref. [7], while the basic models are not fundamentally different from Ref. [7]: all are based on the inherent energy flow equation of heterogeneous energy. Therefore, this section takes the IES case as an example, the existing method [7] and the proposed method are used to establish security region models, the results are compared in the following Table F1 of Appendix F.

From Table F1, it can be seen that the proposed model is much more concise: *s.t.* (1) in the proposed model is equivalent to *s.t.* (1) and *s.t.* (2) in the existing model. The proposed mode is also more unified: in the existing models, the NGS uses a pipeline pressure drop equation, which is significantly different from the EPS; in the proposed model, the NGS uses network equations, which are completely consistent with the form of the EPS. The reason for uniformity is that in the energy circuit model, the form of the electric circuit and the gas circuit are unified.

The unified standardized models of the security region will bring the following benefits.

(1) Possess more in-depth observation and analysis methods across heterogeneous energy subsystems. For example, for example, by calculating the partial derivative of the network matrix, it is easy to discover the influence patterns between specific variables across different subsystems. However, existing methods analyze the interaction between subsystems from the coupling point, which is difficult to achieve the above effect.

(2) The form is consistent with the security region model of EPS, making it easy to draw on a large number of mature methods from EPS and apply them to the analysis of other energy systems.

The similarities and differences between the proposed ECSR and the existing method are summarized in Table I.

TABLE I
SIMILARITIES AND DIFFERENCES AMONG THE PROPOSED ECSR AND EXISTING SECURITY REGION RESEARCH.

	The proposed ECSR	Existing security region research
Similarities	They are all used for security analysis and describe the maximum secure operating range.	
Differences	Security region is modeled based on the network equation described by the energy circuit, the unified modeling of the energy system security region is realized for the first time.	Security region is modeled based on the equilibrium equations of each system, the mathematical models have different forms.
	Offline solution speed of the security region is improved from the model level, the full-dimensional boundary expressions are obtained.	Pay more attention in algorithm improvement, the full-dimensional security boundary expressions are not obtained.

VI. DISCUSSION

For a single energy system, the proposed method is also applicable. In other words, for the ECSRs of single energy systems, such as ECSRs of EPS and NGS, they are only special cases after the degradation of the ECSR of IES.

The proposed method is also applicable to IES composed of other forms of energy, such as thermal energy system and hydrogen energy system. For thermal energy system, the transmission process can also be equivalent to network equations. The equivalent process is detailed in Ref. [16]. For hydrogen energy system, the transmission of hydrogen follows

a network equation similar to natural gas. After obtaining a unified form of network equations, the ECSRs of thermal energy system and hydrogen energy system can be modelled.

In addition, this paper has not yet considered stability, as the security region of this paper mainly focuses on steady state rather than dynamic state. The stability of the security region has been studied in the power system, mainly described through the dynamic security region: the dynamic security region is a set defined in the space of injected power before the fault, when the operating point is in this set, the power system maintains stability even after the expected fault occurs [6]. The dynamic security margin is generally described using the security distance [6], which is the distance from the operating point to the boundary of security region, as a stability indicator. The dynamic security region of power system has important reference significance for the stability analysis of other energy systems. Usually, the operating point is far from the security boundary, and the steady-state region can be used for online analysis, only when the operating point is very close to the boundary, dynamic conditions need to be considered to further improve the analysis accuracy.

VII. Conclusion

In response to the issue of inconsistent security region models caused by the different physical transmission processes and mathematical representations of heterogeneous energy sources, this paper proposes the ECSRs for energy systems. This paper lays the foundation for the research on ECSR, focusing on its conceptualization and modeling. The contributions are summarized as follows:

(1) The concept of ECSR is proposed, with the idea of considering the similarity in network characteristics of heterogeneous energy systems to establish a unified standardized model under certain conditions.

(2) ECSR of EPS, NGS and IES are established respectively, which solves the problem of lacking unified standardized security region models for these different energy systems.

(3) The diagrams of energy circuits for heterogeneous energy systems are first constructed, vividly reflecting the role of network components in energy flow.

(4) The correctness and advantages of the method proposed in this paper are verified through a case of IES, as well as cases of EPS and NGS.

Compared to the existing methods, the proposed method has the following advantages: the model is significantly more concise and unified, it can be applied to both single energy systems and IES. Based on the proposed model, a large number of mature methods of EPS can extend to the analysis of non-electric energy systems, more in-depth observation and analysis methods across heterogeneous energy subsystems can be derived. To verify the universality of ECSR, future work will seek to extend the proposed method to thermal system and hydrogen system, as well as the analysis of dynamic conditions.

Acknowledgment

The authors gratefully acknowledge the National Natural Science Foundation of China (52307079) and the Natural Science Foundation of Hunan Province (2024JJ6050).

References

[1]. H. Sun *et al*., "Integrated energy management system: concept, design, and demonstration in China," *IEEE Elect. Mag.*, vol. 6, no. 2, pp. 42-50, Jun 2018. DOI: 10.1109/MELE.2018.2816842.

[2]. Z. Li *et al*., "Distributed tri-layer risk-averse stochastic game approach for energy trading among multi-energy microgrids," *Appl. Energy*, vol. 331, Feb. 2023, Art. no. 120282. DOI: 10.1016/j.apenergy.2023.120736.

[3]. A. Andrea, C. G. Pedro, G. Blazhe, and S. Giovanni, "Can models for long-term decarbonization policies guarantee security of power supply? A perspective from gas and power sector coupling," *Energy Strateg Rev*., vol. 26, Nov. 2019, Art. no. 100410. DOI: 10.1016/j.esr.2019.100410

[4]. J. Deng, G. Wu, Y. Wang, Y. Su, and A. Liu, "Security-constrained hybrid optimal energy flow model of multi-energy system considering N-1 component failure," *J. Energy Storage*, vol. 64, Aug. 2023, Art. no. 107060. DOI: 10.1016/j.est.2023.107060.

[5]. L. Liu, D. WANG, K. HOU, H. Jia, and S. Li, "Region model and application of regional integrated energy system security analysis," *Appl. Energy*, vol. 260, Feb. 2020, Art. no. 114268. DOI: 10.1016/j.apenergy.2019.114268.

[6]. Y. Yu, Y. Liu, C. Qin, and T. Yang, "Theory and Method of Power System Integrated Security Region Irrelevant to Operation States: An Introduction," *Engineering*, vol. 6, no. 7, pp. 754-777, Jul 2020. DOI: 10.1016/j.eng.2019.11.016.

[7]. S. Chen *et al*., "Steady-state security regions of electricity-gas integrated energy systems," in *Proc. IEEE Power and Energy Soc. Gen. Meeting*, Boston, MA. 2016. pp. 1-5. DOI: 10.1109/PESGM.2016.7741474.

[8]. S. Chen, Z. Wei, G. Sun, W Wei, and D Wang, "Convex hull based robust security region for electricity-gas integrated energy systems," *IEEE Trans. Power Syst*., vol. 34, no. 3, pp. 1740-1748, May 2019. DOI: 10.1109/TPWRS.2018.2888605.

[9]. X. Li, G. Tian, Q. Shi, T. Jiang, F. Li, and H Jia, "Security region of natural gas network in electricity-gas integrated energy system," *Int. J. Electr. Power Energy Syst*., vol. 117, May. 2020, Art. no. 105601. DOI: 10.1016/j.ijepes.2019.105601.

[10]. T. Jiang, R. Zhang, X. Li, H. Chen, and G. Li, "Integrated energy system security region: concepts, methods, and implementations," *Appl. Energy*, vol. 283, Feb. 2021, Art. no. 116124. DOI: 10.1016/j.apenergy.2020.116124.

[11]. J. Su, H.-D. Chiang, and F. C. A. Luís, "Two-time-scale approach to characterize the steady-state security region for the electricity-gas integrated energy system," *IEEE Trans. Power Syst*., vol. 36, no. 6, pp. 5863-5873, Nov. 2021. DOI: 10.1109/TPWRS.2021.3081700.

[12]. J. Su, H.-D. Chiang, Y. Zeng, and N. Zhou, "Toward complete characterization of the steady-state security region for the electricity-gas integrated energy system," *IEEE Trans. Smart Grid*, vol. 12, no. 4, pp. 3004-3015, Jul. 2021. DOI: 10.1109/TSG.2021.3065501.

[13]. P. Yong, Y. Wang, T. Capuder, Z. Tan, N. Zhang, and C. Kang, "Steady-state security region of energy hub: Modeling, calculation, and applications," *Int. J. Elect. Power Energy Syst*., vol. 125, Feb. 2021, Art. no. 106551. DOI: 10.1016/j.ijepes.2020.106551.

[14]. S. Zhang, W. Gu, X. Zhang, S. Lu, G. Pan, and S. Ding, "Steady-state security region of integrated energy system considering thermal dynamics," *IEEE Trans. Power Syst*., vol. 38, no. 2, pp. 1651-1654, Mar. 2023. DOI: 10.1109/TPWRS.2023.3296080.

[15]. H. Ma, C. Liu, H. Zhao, H. Zhang, M. Wang, and X. Wang, "A novel analytical unified energy flow calculation method for integrated energy systems based on holomorphic embedding," *Appl. Energy*, vol. 344, Feb. 2023, Art. no. 120163. DOI: 0.1016/j.apenergy.2023.121163.

[16]. B. Chen, Q. Guo, G. Yin, B. Wang, Z. Pan, Y. Chen, et al., "Energy-circuit-based integrated energy management system: Theory, implementation, and application," *Proc. IEEE*, vol. 110, no. 12, pp. 1897-1926, Dec. 2022. DOI: 10.1109/JPROC.2022.3216567.

[17]. B. Chen, W. Wu, Q. Guo, and H. Sun, "An efficient optimal energy flow model for integrated energy systems based on energy circuit modeling in

the frequency domain," *Appl. Energy*, vol. 326, Nov. 2022, Art. no. 119923. DOI: 10.1016/j.apenergy.2022.119923.
[18]. B. Chen, H. Sun, Y. Chen, W. Wu, and Z. Qiao, "Energy circuit theory of integrated energy system analysis (I): Gaseous circuit," *Proc. CSEE (in Chinese)*, vol. 40, no. 2, pp. 436-444, Jan. 2020. DOI: 10.13334/j.0258-8013.pcsee.200028.
[19]. B. Chen, H. Sun, G. Yin, W. Wu, Q. Guo, Y. Chen, et al., "Energy circuit theory of integrated energy system analysis (II): Hydraulic circuit and thermal circuit," *Proc. CSEE (in Chinese)*, vol. 40, no. 7, pp. 2133-2142, Mar. 2020. DOI: 10.13334/j.0258-8013.pcsee.200098.
[20]. B. Chen, H. Sun, W. Wu, Q. Guo, and Z. Qiao, "Energy circuit theory of integrated energy system analysis (III): Steady and dynamic energy flow calculation," *Proc. CSEE (in Chinese)*, vol. 40, no. 15, pp. 4820-4831, Jul. 2020. DOI: 10.13334/j.0258-8013.pcsee.200647.
[21]. G. Yin, B. Chen, H. Sun, and Q. Guo, "Energy circuit theory of integrated energy system analysis (IV): Dynamic state estimation of the natural gas network," *Proc. CSEE (in Chinese)*, vol. 40, no. 18, pp. 5827-5837, Aug. 2020. DOI: 10.13334/j.0258-8013.pcsee.200731.
[22]. Y. Chen, H. Sun, and Q. Guo, "Energy circuit theory of integrated energy system analysis (V): Integrated electricity-heat-gas dispatch," *Proc. CSEE (in Chinese)*, vol. 40, no. 24, pp. 7928-7937, Dec. 2020. DOI: 10.13334/j.0258-8013.pcsee.201715.
[23]. J. Yang, N. Zhang, A. Botterud, and C. Kang, "Situation awareness of electricity-gas coupled systems with a multi-port equivalent gas network model," *Appl. Energy*, vol. 258, Jan. 2020, Art. no. 114029. DOI: 10.1016/j.apenergy.2019.114029.
[24]. J. Yang, N. Zhang, and C. Kang, "Analysis theory of generalized electric circuit for multi-energy networks—Part one: Branch model," *Autom. Electr. Power Syst. (in Chinese)*, vol. 44, no. 9, pp. 21-32, May 2020. DOI: 10. 7500/AEPS20200209001.
[25]. J. Yang, N. Zhang, and C. Kang, "Analysis theory of generalized electric circuit for multi-energy networks—Part two: Network model," *Autom. Electr. Power Syst. (in Chinese)*, vol. 44, no. 10, pp. 10-21, May 2020. DOI: 10. 7500/AEPS20200209002.
[26]. J. Chen, F. Li, H. Li, B. Sun, C. Zhang, and S. Liu, "Novel dynamic equivalent circuit model of integrated energy systems," *Energy*, vol. 262, Jan. 2023, Art. no. 125266. DOI: 10.1016/j.energy.2022.125266.
[27]. L. Wang, J. Zheng, Z. Li, Z. Jing, and Q. Wu, "Order reduction method for high-order dynamic analysis of heterogeneous integrated energy systems," *Appl. Energy*, vol. 308, Feb. 2022, Art. no. 118265. DOI: 10.1016/j.apenergy.2021.118265.
[28]. S. Zhang, W. Gu, S. Yao, S. Zhou, and Z. Wu, "Unified modeling of integrated energy networks in time domain and its applications (I): Two-part models in time domain," *Proc. CSEE (in Chinese)*, vol. 41, no. 19, pp. 6509-6521, Jul. 2021. DOI: 10.13334/j.0258-8013.pcsee.210486.
[29]. Y. Qu, J. Xiao, and G. Zu, "Security region and power supply capability for distribution system under normal operational state: Definition, model, and application," *CSEE J. Power Energy Syst*., to be published. DOI: 10.17775/CSEEJPES.2022.04140.
[30]. Z. Wu, Q. Sun, Y. Lu, W. Gu, P. Liu, et al., "Distributed chance-constrained based total energy supply capability evaluation method for integrated power and natural gas system," *Int. J. Electr. Power Energy Syst*., vol. 141, Oct 2022, Art. no. 108193. DOI: 10.1016/j.ijepes.2022.108193.
[31]. J. Xiao, X. Lin, H. Jiao, C. Song, H. Zhou, et al., "Model, calculation, and application of available supply capability for distribution systems," *Appl. Energy,* vol. 348, Oct 2023, Art. no. 121489. DOI: 10.1016/j.apenergy.2019.114268.
[32]. J. Xiao, C. Song, G. Zu, L. Lv, B. She, et al., "Gas transmission capability curve of natural gas system: Concept and steady-state model," *J. Nat. Gas Sci. Eng*., vol. 87, Mar 2021, Art. no. 103754. DOI: 10.1016/j.jngse.2020.103754.
[33]. C. Song, J. Xiao, G. Zu, Z. Hao, and X. Zhang, "Security region of natural gas pipeline network system: Concept, method and application," *Energy*, vol. 217, Feb 2021, Art. no. 119283. DOI: 10.1016/j.energy.2020.119283.
[34]. G. H. Golub and C. F. Van Loan, *Matrix Computations*. 4th ed. Baltimore, MD, USA: Johns Hopkins Univ. Press, 2013.

APPENDIX

A. Nomenclature

TABLE A1
LIST OF THE ACRONYMS IN THIS PAPER.

Symbol	Meaning
EPS	electric power system
NGS	natural gas system
IES	integrated energy system
IES-SR	security region of integrated energy system
EPS-SR	security region of electric power system
NGS-SR	security region of natural gas system
ECSR	security region of energy circuit
GT	Gas turbine generator/ Gas generator

TABLE A2
LIST OF THE VARIABLES IN THIS PAPER.

	Symbol	Meaning
Symbols of security region modeling	$\boldsymbol{\Omega}_{\mathrm{SR}}$	generalized symbols for security region
	$\boldsymbol{\Omega}_{\text{EPS-ECSR}}$	ECSR of EPS
	$\boldsymbol{\Omega}_{\text{NGS-ECSR}}$	ECSR of NGS
	$\boldsymbol{\Omega}_{\text{IES-ECSR}}$	ECSR of IES
	$\partial\boldsymbol{\Omega}_{\mathrm{SR}}$	generalized symbols for security boundary
	G_{GTC}	total gas transmission at GTC point
	$\boldsymbol{W}$	operating point
	$\boldsymbol{W}_{\mathrm{s}}$	security operating point
	$\boldsymbol{W}_{\mathrm{b}}$	critical security operating point
	$S_{\mathrm{l},ci}$	power of power load node i
	$S_{\mathrm{l},cm}$	power required to drive compressor m
	$\boldsymbol{I}_{\mathrm{n}}$	vector of node current
	$\boldsymbol{I}_{\mathrm{n}}^{\max}$	vectors of the upper limits of node current
	$\boldsymbol{I}_{\mathrm{n}}^{\min}$	vectors of the lower limits of node current
	$\boldsymbol{I}_{\mathrm{b}}$	vector of branch current
	$\boldsymbol{I}_{\mathrm{b}}^{\max}$	vector of the current-carrying capacity
	$\boldsymbol{U}_{\mathrm{n}}$	vector of node voltage
	$\boldsymbol{U}_{\mathrm{n}}^{\max}$	vectors of the upper limits of node voltage
	$\boldsymbol{U}_{\mathrm{n}}^{\min}$	vectors of the lower limits of node voltage
	$\boldsymbol{K}_{\mathrm{c}}$	transformer ratio matrix
	$G_{\mathrm{l},gj}$	flow rate of natural gas load node j
	$G_{\mathrm{l,GT}n}$	natural gas input by the gas generator n
	$\boldsymbol{G}_{\mathrm{n}}$	vectors of node flow of natural gas
	$\boldsymbol{G}_{\mathrm{n}}^{\max}$	vector of the upper limits of the node gas flow
	$\boldsymbol{G}_{\mathrm{n}}^{\min}$	vector of the lower limits of the node gas flow
	$\boldsymbol{p}_{\mathrm{n}}$	vector of node pressure of natural gas
	$\boldsymbol{p}_{\mathrm{n}}^{\max}$	vector of the upper limits of node pressure
	$\boldsymbol{p}_{\mathrm{n}}^{\min}$	vector of the lower limits of node pressure
	$\boldsymbol{G}_{\mathrm{b}}^{\max}$	vector of pipe capacity
	$\boldsymbol{P}_{\mathrm{n}}$	vector of node pressure
	$\boldsymbol{P}_{\mathrm{n}}^{\max}$	vector of the upper limits of node pressure
	$\boldsymbol{P}_{\mathrm{n}}^{\min}$	vector of the lower limits of node pressure
	$\boldsymbol{F}_{\mathrm{n}}$	vector of energy flow
	$\boldsymbol{F}_{\mathrm{n}}^{\max}$	vector of the upper limits of node flow
	$\boldsymbol{F}_{\mathrm{n}}^{\min}$	vector of the lower limits of node flow
	$\boldsymbol{F}_{\mathrm{b}}^{\max}$	vector of upper limit of allowable flow of branch
	$\boldsymbol{K}$	generalized energy transformation ratio matrix
Symbols of network topology	$\boldsymbol{A}_{\mathrm{g}}$	node-branch incident matrix of NGS
	$\boldsymbol{A}_{\mathrm{g,L}}^{-1}$	Left inverse matrix of $\boldsymbol{A}_{\mathrm{g}}$
	$\boldsymbol{A}_{\mathrm{g}+}$	node-outflow branch incident matrix of NGS
	$\boldsymbol{A}_{\mathrm{g}-}$	node-inflow branch incident matrix of NGS

Symbols of natural gas and pipe parameter	R	constant of natural gas
	T	temperature of natural gas
	v_b	basic value of gas flow rate
	Z	compression factor of natural gas
	κ	adiabatic constant of natural gas
	V_{GH}	total calorific value of natural gas
	g	acceleration of gravity
	ρ	density of natural gas
	d_g	inner diameter of pipe
	s_g	cross-sectional area of pipe
	l_g	length of pipe
	λ_g	friction coefficient of pipe
	θ_g	inclination angle of pipe
Symbols of energy circuit	r_g	gas resistance (distributed parameter)
	L_g	gas inductance (distributed parameter)
	C_g	gas capacitance (distributed parameter)
	k_g	controlled pressure source (distributed parameter)
	Z_{gb}	branch impedance
	k_{gb}	controlled gas pressure source
	$Y_{gb,10}$	ground admittance
	$Y_{gb,20}$	ground admittance
	$\boldsymbol{y}_{gb}$	diagonal matrices of branch admittance (concentrated parameter)
	$\boldsymbol{k}_{gb}$	diagonal matrices of controlled gas pressure source (concentrated parameter)
	$\boldsymbol{Y}_g$	generalized node admittance matrix of NGS
	$\boldsymbol{Y}_e$	node admittance matrix of EPS
	$\boldsymbol{Y}_{IES}$	generalized node admittance matrix of IES
Symbols of coupling unit	ψ	efficiency of compressor
	K_g	pressure ratio of compressor
	$\boldsymbol{K}_g$	matrix of compressor pressure ratio
	a_{GT}	heat consumption coefficients of gas generator
	b_{GT}	heat consumption coefficients of gas generator
	c_{GT}	heat consumption coefficients of gas generator
	d_{GT}	heat consumption coefficients of gas generator
	e_{GT}	heat consumption coefficients of gas generator
	P_{GT}	active power output by the gas generator
	P_{GT}^{min}	lower limit of P_{GT}

TABLE A3
GIVEN QUANTITIES AND STATE VARIABLES OF DIFFERENT ENERGY SYSTEMS.

	Given quantities	State variables
Power system	$\boldsymbol{I}_n^{max}$, $\boldsymbol{I}_n^{min}$, $\boldsymbol{U}_n^{max}$, $\boldsymbol{U}_n^{min}$, $\boldsymbol{S}_b^{max}$, K_e	$\boldsymbol{W}$, $S_{l,ci}$, $S_{l,ci}$, $\boldsymbol{I}_n$, $\boldsymbol{U}_n$, $\boldsymbol{S}_b$, P_{GT}
Natural gas system	$\boldsymbol{G}_n^{max}$, $\boldsymbol{G}_n^{min}$, $\boldsymbol{p}_n^{max}$, $\boldsymbol{p}_n^{min}$, $\boldsymbol{G}_b^{max}$, K, η	$\boldsymbol{W}$, $G_{l,gj}$, $G_{l,GTj}$, $\boldsymbol{G}_n$, $\boldsymbol{p}_n$, $\boldsymbol{G}_b$
Integrated energy system	$\boldsymbol{P}_n^{max}$, $\boldsymbol{P}_n^{min}$, $\boldsymbol{F}_n^{max}$, $\boldsymbol{F}_n^{min}$, $\boldsymbol{F}_b^{max}$, P_{GT}^{min}, a_{GT}, b_{GT}, c_{GT}, d_{GT}, e_{GT}, K, η	$\boldsymbol{W}$, $\boldsymbol{P}_n$, $\boldsymbol{F}_n$, $\boldsymbol{F}_b$

B. The derivation process of gas circuit and network equation modeling in NGS

1) Derivation process of steady-state gas circuit of pipe

First, linearize the momentum conservation equation of NGS, the process is as follows.

(1) The natural gas flow in pipelines can be described by the mass conservation equation shown in equation (B1) and the momentum conservation equation shown in equation (B2),

$$\frac{\partial \rho}{\partial t}+\frac{\partial \rho v}{\partial x}=0 \tag{B1}$$

$$\frac{\partial \rho v}{\partial t}+\frac{\partial \rho v^2}{\partial x}+\frac{\partial p}{\partial x}+\frac{\lambda_g \rho v^2}{2d_g}+\rho g\sin\theta_g=0 \tag{B2}$$

where, v and ρ represent the actual flow rate and pressure of natural gas; ∂t and ∂x represent partial differentials for time and space.

(2) Two commonly approximations in engineering are introduced for the above momentum conservation equation.

1) Ignore the convection term in equation (B2), as shown in equation (B3):

$$\frac{\partial \rho v^2}{\partial x}=0 \tag{B3}$$

2) Linearize and approximate the square term of flow velocity in the resistance term of equation (B2), as shown in equation (B4):

$$v^2=\left(v_b+\Delta v\right)^2\approx v_b^2+2v_b\Delta v=2v_b v-v_b^2 \tag{B4}$$

where, Δv is the fluctuation of the actual flow rate "v" relative to the basic value of flow rate "v_b" of natural gas.

Then, the resistance term in equation (B2) can be expressed as a linear function of flow velocity, as shown in equation (B5).

$$\frac{\lambda_g \rho v^2}{2d_g}\approx\frac{\lambda_g \rho\left(2v_b v-v_b^2\right)}{2d_g} \tag{B5}$$

Second, establish a gas circuit model of distributed parameter for natural gas pipeline, the process is as follows.

(1) Introduce the state equation of natural gas, as shown in equation (B6),

$$p=RT\rho Z \tag{B6}$$

where, "Z", thus the compression factor of natural gas is generally taken as 1.

(2) Introduce the mass flow rate of natural gas, as shown in equation (B7):

$$G=\rho v s_g \tag{B7}$$

where, G is the mass flow rate of natural gas.

(3) Substitute equations (B3)~(B7) into equations (B1)~(B2), the partial differential equations, which describes the relationship between natural gas flow and pressure of pipelines, can be obtained, as shown in equations (B8) and (B9):

$$s_g\frac{\partial p}{\partial t}+RT\frac{\partial G}{\partial x}=0 \tag{B8}$$

$$\frac{1}{s_g}\frac{\partial G}{\partial t}+\frac{\partial p}{\partial x}+\frac{\lambda_g v_b p}{2RTd_g}+\frac{pg\sin\theta_g}{RT}=0 \tag{B9}$$

(4) According to equations (B8) and (B9), the flow difference and pressure difference at both ends of a micro element pipeline with the length of "dx" are expressed as equations (B10) and (B11):

$$\mathrm{d}G=-\frac{s_g}{RT}\cdot\frac{\mathrm{d}p}{\mathrm{d}t}\cdot\mathrm{d}x \tag{B10}$$

$$\mathrm{d}G=-\frac{s_g}{RT}\cdot\frac{\mathrm{d}p}{\mathrm{d}t}\cdot\mathrm{d}x \tag{B11}$$

(5) Make an analogy between the pressure at both ends of natural gas pipeline with the flow through it and the voltage at both ends of electric branch with the current through it. Like the circuit, the distributed parameter model of gas circuit shown in Figure B1, as well as the gas resistance r_g, gas inductance L_g, controlled pressure source k_g and gas capacitance C_g in the model, can be sorted out from the equations (B10) and (B11).

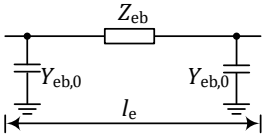

Fig. B1. Distributed parameter model of gas circuit of pipeline

At steady state, by treating the gas inductance as a "short circuit" and the gas capacitance as an "open circuit", the calculation equations for the components of the gas circuit in the form of distributed parameter shown in equations (5)~(8) in section 3.2.2 can be obtained.

$$r_g = \frac{\lambda_g v_b}{s_g d_g} \tag{B12}$$

$$L_g = 0 \tag{B13}$$

$$k_g = \frac{2gd_g \sin\theta_g - \lambda_g v_b^2}{2RTs_g} \tag{B14}$$

$$C_g = 0 \tag{B15}$$

Third, the gas circuit model in centralized parameters of natural gas pipeline is established, the process is as follows.

(1) Substituting equations (B12)~(B15) into equations (B10) and (B11), the flow difference and pressure difference at both ends of a micro element pipeline with the length of "dx" in steady-state can be expressed as equations (B16) and (B17).

$$\mathrm{d}G = -C_g \cdot \mathrm{d}x \cdot \mathrm{d}p/\mathrm{d}t = 0 \tag{B16}$$

$$\begin{aligned} \mathrm{d}p &= -L_g \cdot \mathrm{d}x \cdot \mathrm{d}G/\mathrm{d}t - r_g \cdot \mathrm{d}x \cdot G - k_g \cdot \mathrm{d}x \cdot p \\ &= -r_g \cdot \mathrm{d}x \cdot G - k_g \cdot \mathrm{d}x \cdot p \end{aligned} \tag{B17}$$

(2) Mapping equations (B16) and (B17) to the frequency domain, as well as adding boundary conditions for the flow and pressure of the head end of pipe: $G|_{x=0}=G_0$, $p|_{x=0}=p_0$, the flow rate G_l and pressure p_l of the end of a pipeline with a length of l_g can be obtained, as shown in equations (B18) and (B19).

$$G_l = G_0 \tag{B18}$$

$$p_l = [p_0(\cosh\frac{k_g l_g}{2} - \sinh\frac{k_g l_g}{2}) - G_0\frac{2r_g}{k_g}\sinh\frac{k_g l_g}{2}]e^{-\frac{k_g l_g}{2}} \tag{B19}$$

(3) Express the gas flow and pressure at the beginning and end of the pipeline as a two-port network.

$$\begin{bmatrix} p_l \\ G_l \end{bmatrix} = \begin{bmatrix} A & B \\ C & D \end{bmatrix}\begin{bmatrix} p_0 \\ G_0 \end{bmatrix} \tag{B20}$$

At steady state, the parameters of the two-port network are shown in equations (B21)~(B24).

$$A = (\cosh\frac{k_g l_g}{2} - \sinh\frac{k_g l_g}{2})e^{-\frac{k_g l_g}{2}} \tag{B21}$$

$$B = -2\frac{r_g}{k_g} \cdot \sinh\frac{k_g l_g}{2} \cdot e^{-\frac{k_g l_g}{2}} \tag{B22}$$

$$C = 0 \tag{B23}$$

$$D = 1 \tag{B24}$$

(4) Base on the two-port network shown in equations (B21)~(B24), the concentrated parameter model in the form of π-type equivalent gas circuit shown in Figure B2, as well as the branch impedance Z_{gb}, controlled pressure source k_{gb}, ground admittance $Y_{gb,10}$ and $Y_{gb,20}$, can be obtained.

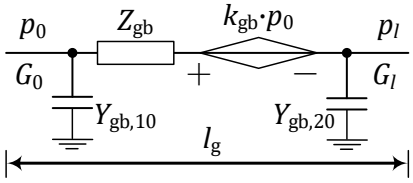

Fig. B2. Concentrated parameter model of gas circuit of pipeline

At steady state, by organizing equations (B21)~(B24), the calculation equation for the components of the π-type gas circuit in the form of concentrated parameter shown in equations (9)~(12) in section 3.2.2 can be obtained.

$$Z_{gb} = -B = 2\frac{r_g}{k_g} \cdot \sinh\frac{k_g l_g}{2} \cdot e^{-\frac{k_g l_g}{2}} \tag{B25}$$

$$k_{gb} = 1 - AD + BC = (\cosh\frac{k_g l_g}{2} - \sinh\frac{k_g l_g}{2})e^{-\frac{k_g l_g}{2}} \tag{B26}$$

$$Y_{gb,10} = (AD - BC - A)/B = 0 \tag{B27}$$

$$Y_{gb,20} = (1 - D)/B = 0 \tag{B28}$$

2) Derivation process of steady-state network equation

Based on the concentrated parameter model of gas circuit of pipeline, considering the branches characteristics and network topology of NGS, the network equations of NGS shown in equation (13) in section 3.2.2 can be obtained. The specific process is as follows.

First, considering the branch characteristics of the NGS, that is, to model the pipeline branch with a compressor.

(1) For compressor modeling, Ref. [16] equates it to a gas pressure source during modeling, which has the advantage of simplicity and intuition, but the description of actual operation is somewhat ideal. In the field of natural gas, using compressor pressure ratio to simulate pressure changes in pipelines containing compressors is a more common modeling method [24], which is more in line with the operating characteristics of compressors. In the generalized electric circuit theory, a similar modeling method is adopted considering that compressors in NGS and transformers in EPS have similar boosting functions [24]. This paper draws inspiration from Ref. [24], equates the compressor to a gas circuit transformer, as shown in equation (B29):

$$p_{c'} = K_g p_c \tag{B29}$$

where , p_c and $p_{c'}$ are the pressures at the beginning and end of the compressor, K_g is the pressure ratio of compressor.

(2) Based on equation (B29) and the π-type equivalent gas circuit of pipeline in steady-state, the gas circuit of the pipeline branch with a compressor in steady-state can be represented in the form of Figure B3. In the figure, p_f and p_t are the pressures at the beginning and end of pipeline; Z_{gb} and Y_{gb} are the impedance and admittance of pipeline, they use steady-state values of the parameters of π-type equivalent gas circuit; K_{gb} is the controlled gas pressure source of pipeline; G_b and P_b represent the natural gas flow and pressure drop of pipeline.

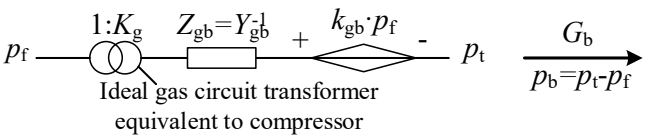

Fig. B3. steady-state gas circuit of pipeline with a compressor

Obviously, the pipeline with compressor shown in Figure B3 satisfies the equation shown in equation (B30).

$$p_f \cdot K_g - G_b \cdot Z_{gb} - k_{gb} \cdot p_f = p_t \tag{B30}$$

(3) By using branch admittance Y_{gb} to represent branch impedance Z_{gb} and organizing equation (B30), the steady-state gas pipeline equation considering branch characteristics can be obtained, as shown in equation (B31).

$$Y_{gb} \cdot (K_g \cdot p_f - k_{gb} \cdot p_f - p_t) = G_b \tag{B31}$$

Further, the matrix form of equation (B31) is as follows,

$$\boldsymbol{Y}_{gb}(\boldsymbol{K}\boldsymbol{p}_f - \boldsymbol{k}_{gb}\boldsymbol{p}_f - \boldsymbol{p}_t) = \boldsymbol{G}_b \tag{B32}$$

where, $\boldsymbol{p}_f$, $\boldsymbol{p}_t$ and $\boldsymbol{G}_b$ are vectors composed of p_f, p_t, and G_b.

Second, based on the branch characteristics, consider the network topology characteristics of NGS further.

(1) To describe the network topology, the node-branch incident matrix $\boldsymbol{A}_g$, node-outflow branch incident matrix $\boldsymbol{A}_{g+}$, and node-inflow branch incident matrix $\boldsymbol{A}_{g-}$ of NGS are introduced. At the same time, it is specified that the outflow direction at the load node is positive.

The meanings and forms of $\boldsymbol{A}_g$, $\boldsymbol{A}_{g+}$ and $\boldsymbol{A}_{g-}$ are as follows.

$\boldsymbol{A}_g$ is a matrix that describes the relationship between nodes and branches, its concept originated from EPS. For a NGS with m nodes and n pipelines, $\boldsymbol{A}_g$ is represented as a matrix of m rows and n columns. Use $(\boldsymbol{A}_g)_{i,j}$ to represent the element in the i-th row and j-th column of Ag. $(\boldsymbol{A}_g)_{i,j}$=0 means that branch j is not connected to node i; $(\boldsymbol{A}_g)_{i,j}$=1 means that the traffic flow out of node i from branch j; $(\boldsymbol{A}_g)_{i,j}$=-1 means that traffic flow from branch j into node i.

$\boldsymbol{A}_{g+}$ is a matrix that describes the relationship between nodes and outflow pipeline branches. $\boldsymbol{A}_{g+}$ only retains non-negative elements of $\boldsymbol{A}_g$, that is, for $(\boldsymbol{A}_{g+})_{i,j}$, if the traffic flow out of node i through branch j, $(\boldsymbol{A}_{g+})_{i,j}$=1, otherwise $(\boldsymbol{A}_{g+})_{i,j}$=0.

$\boldsymbol{A}_{g-}$ is a matrix that describes the relationship between nodes and inflow pipeline. $\boldsymbol{A}_{g-}$ only retains non-positive elements of $\boldsymbol{A}_g$, that is, for $(\boldsymbol{A}_{g-})_{i,j}$, if the traffic flow out of node i through branch j, $(\boldsymbol{A}_{g-})_{i,j}$=1, otherwise $(\boldsymbol{A}_{g+})_{i,j}$=0.

(2) According to Kirchhoff law, the flow and gas pressure of nodes and branches of NGS satisfy the relationship shown in equations (B33)~(B35).

$$-\boldsymbol{A}_g^T \boldsymbol{G}_b = \boldsymbol{G}_n \tag{B33}$$

$$Y_{gb,10} = (AD - BC - A)/B = 0 \tag{B34}$$

$$Y_{gb,20} = (1 - D)/B = 0 \tag{B35}$$

(3) Substituting equations (B33)~(B35) into equation (B32), the network equation of NGS will be obtained, as shown in equation (B36).

$$\boldsymbol{G}_n = -\boldsymbol{A}_g \boldsymbol{Y}_{gb}(\boldsymbol{K}_g \boldsymbol{A}_{g+}^T \boldsymbol{p}_n - \boldsymbol{k}_{gb} \boldsymbol{A}_{g+}^T \boldsymbol{p}_n - \boldsymbol{A}_{g-}^T \boldsymbol{p}_n) \tag{B36}$$

(4) Introduce the generalized node admittance matrix of NGS $\boldsymbol{Y}_g$ as follows,

$$\boldsymbol{Y}_g = -\boldsymbol{A}_g \boldsymbol{Y}_{gb}(\boldsymbol{K}_g \boldsymbol{A}_{g+}^T - \boldsymbol{k}_{gb} \boldsymbol{A}_{g+}^T - \boldsymbol{A}_{g-}^T) \tag{B37}$$

then the network equation in the form of equation (B37) can be organized into the form shown in equation (10) in section 3.2.2. Thus, the network equation of NGS, which is consistent with the form of the network equation of EPS is obtained, as shown in equation (B38):

$$\boldsymbol{Y}_g \boldsymbol{p}_n = \boldsymbol{G}_n \tag{B38}$$

C. Method for setting the basic value of gas flow rate of NGS

The principle for setting the base value of gas flow rate is to be as close as possible to the actual flow rate of the pipeline, because the smaller the fluctuation of the actual flow rate relative to the base value, the smaller the error introduced in theory [18,20].

There are two problems about setting the base value: (1) for different operating points, the corresponding pipeline flow rate varies greatly. If the base value is set to the same value, it will introduce significant errors; (2) for each pipe segment with different pipe diameters, using the same base value will also introduce errors. Therefore, this paper takes into account both of these issues when taking values. The equation for the base value is as follows:

$$\boldsymbol{v}_b = -\boldsymbol{A}_{g,L}^{-1} \boldsymbol{G}_n \big/ \boldsymbol{s}\rho \tag{C1}$$

where, $\boldsymbol{v}_b$ represents the vector of base value of gas flow rate; $\boldsymbol{A}_{g,L}^{-1}$ represents the Left inverse matrix of $\boldsymbol{A}_g$ [20], which can be obtained by $\boldsymbol{A}_g$ through matrix transformation; $\boldsymbol{G}_n$ represents the vector of the mass flow rate of natural gas injected into each node; $\boldsymbol{s}$ represents the vector of the diameters of each pipe; ρ is the density of natural gas (if volumetric flow is used, ρ will not need to be included).

It needs to be explained further.

(1) The above basic value setting process is mainly aimed at static state. If transient conditions are considered, the base value can be taken as the steady-state value at the initial time [20].

(2) After setting the basic value v_b, the network equation of NGS is linear. When it is difficult to ensure the base value is close enough to the actual flow rate, the base value can be corrected through iterative calculation to improve accuracy [20].

D. Derivation process of ECSR of IES

(1) First, the ECSR of EPS is taken as constraint *s.t.* (D1-1). Second, the ECSR of NGSS is taken as constraint *s.t.* (D1-2). Third, for the coupling units, they are compressor and gas generator in this paper, take the constraints of coupling units as constraint *s.t.* (D1-3). Finally, according to the constraints s.*t.* (D1-1)~*s.t.* (D1-3), the security region model shown in equation (D1) can be obtained:

$$\begin{cases} \boldsymbol{\Omega}_{\text{IES-SR}} = \left\{ \boldsymbol{W}_{\text{s}} \middle| \boldsymbol{h}(\boldsymbol{W}_{\text{s}}) = \boldsymbol{0}, \boldsymbol{g}(\boldsymbol{W}_{\text{s}}) \le \boldsymbol{0} \right\} \\ s.t.(\text{D1}-1) \begin{cases} \boldsymbol{Y}_{\text{e}} \boldsymbol{U}_{\text{n}} = \boldsymbol{I}_{\text{n}} \\ \boldsymbol{U}_{\text{n}}^{\min} \le \boldsymbol{U}_{\text{n}} \le \boldsymbol{U}_{\text{n}}^{\max} \\ \boldsymbol{I}_{\text{n}}^{\min} \le \boldsymbol{I}_{\text{n}} \le \boldsymbol{I}_{\text{n}}^{\max} \\ \boldsymbol{I}_{\text{b}} \le \boldsymbol{I}_{\text{b}}^{\max} \\ \boldsymbol{K}_{\text{e}}^{\min} \le \boldsymbol{K}_{\text{e}} \le \boldsymbol{K}_{\text{e}}^{\max} \end{cases} \\ s.t.(\text{D1}-2) \begin{cases} \boldsymbol{Y}_{\text{g}} \boldsymbol{p}_{\text{n}} = \boldsymbol{G}_{\text{n}} \\ \boldsymbol{p}_{\text{n}}^{\min} \le \boldsymbol{p}_{\text{n}} \le \boldsymbol{p}_{\text{n}}^{\max} \\ \boldsymbol{G}_{\text{n}}^{\min} \le \boldsymbol{G}_{\text{n}} \le \boldsymbol{G}_{\text{n}}^{\max} \\ \boldsymbol{G}_{\text{b}} \le \boldsymbol{G}_{\text{b}}^{\max} \\ \boldsymbol{K}_{\text{g}}^{\min} \le \boldsymbol{K}_{\text{g}} \le \boldsymbol{K}_{\text{g}}^{\max} \end{cases} \\ s.t.(\text{D1}-3) \begin{cases} S_{\text{c}} = \dfrac{151.4653 p_0 Z T G_c \kappa}{\psi T_0 (\kappa \text{-} 1)} (K_{\text{g}}^{\frac{\kappa}{\kappa\text{-}1}} - 1) \\ G_{\text{GT}} = \dfrac{1}{\text{V}_{\text{GH}}} (a_{\text{GT}} P_{GT}^2 + b_{\text{GT}} P_{GT} + c_{\text{GT}} + \left| d_{\text{GT}} \sin(e_{\text{GT}} (P_{\text{GT}}^{\min} - P_{GT})) \right|) \end{cases} \end{cases} \tag{D1}$$

(2) Combine the node admittance matrix of EPS "$\boldsymbol{Y}_{\text{e}}$" and the node admittance matrix of NGS "$\boldsymbol{Y}_{\text{g}}$" to form the node admittance matrix of IES "$\boldsymbol{Y}_{\text{IES}}$" in blocks. Combine voltage and gas pressure to form the pressure vector of IES "$\boldsymbol{P}_{\text{n}}$". Combine current and gas flow to form the flow vector of IES "$\boldsymbol{F}_{\text{n}}$". Combine the transformer ratio matrix "$\boldsymbol{K}_{\text{e}}$" and the compressor pressure ratio matrix "$\boldsymbol{K}_{\text{g}}$" to form a generalized energy ratio matrix "$\boldsymbol{K}$".

(3) By combining *s.t.* (D1-1) and *s.t.* (D1-2) in equation (D1) to form *s.t.* (D2-1) in equation (D2), taking *s.t.* (D1-1) in equation (D1) as *s.t.* (D2-2) in equation (D2), the ECSR of IES shown in equation (D2) can be obtained:

$$\begin{cases} \boldsymbol{\Omega}_{\text{IES-SR}} = \left\{ \boldsymbol{W}_{\text{s}} \middle| \boldsymbol{h}(\boldsymbol{W}_{\text{s}}) = \boldsymbol{0}, \boldsymbol{g}(\boldsymbol{W}_{\text{s}}) \le \boldsymbol{0} \right\} \\ s.t.(\text{D2}-1) \begin{cases} \boldsymbol{Y}_{\text{IES}} \boldsymbol{P}_{\text{n}} = \boldsymbol{F}_{\text{n}} \\ \boldsymbol{P}_{\text{n}}^{\min} \le \boldsymbol{P}_{\text{n}} \le \boldsymbol{P}_{\text{n}}^{\max} \\ \boldsymbol{F}_{\text{n}}^{\min} \le \boldsymbol{F}_{\text{n}} \le \boldsymbol{F}_{\text{n}}^{\max} \\ \boldsymbol{F}_{\text{b}} \le \boldsymbol{F}_{\text{b}}^{\max} \\ \boldsymbol{K}^{\min} \le \boldsymbol{K}_{\text{e}} \le \boldsymbol{K}^{\max} \end{cases} \\ s.t.(\text{D2}-2) \begin{cases} S_{\text{c}} = \dfrac{151.4653 p_0 Z T G_c \kappa}{\psi T_0 (\kappa \text{-} 1)} (K_{\text{g}}^{\frac{\kappa}{\kappa\text{-}1}} - 1) \\ G_{\text{GT}} = \dfrac{1}{\text{V}_{\text{GH}}} (a_{\text{GT}} P_{GT}^2 + b_{\text{GT}} P_{GT} + c_{\text{GT}} + \left| d_{\text{GT}} \sin(e_{\text{GT}} (P_{\text{GT}}^{\min} - P_{GT})) \right|) \end{cases} \end{cases} \tag{D2}$$

E. Structure and detailed parameters of the cases

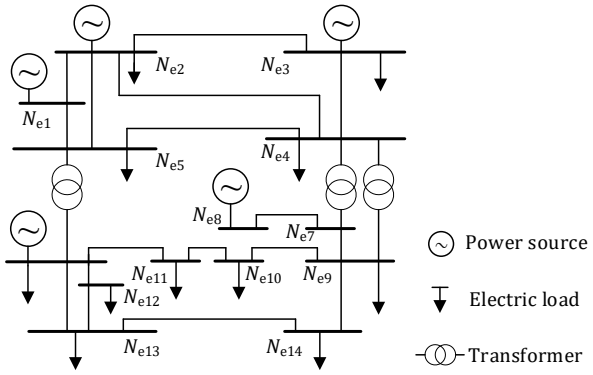

Fig. E1 Structure of IEEE 14-bus system

TABLE E1

BUS PARAMETERS OF IEEE 14-BUS EPS.

Bus	Bus type	Bus Voltage range (p.u.)	Generator active power range (MW)	Generator reactive power range (MVar)	Load apparent power range (MVA)	Load power factor
N_{e1}	slack bus	1.06	[0, 250]	[-10, 10]	-	-
N_{e2}	PV bus	1.045	[0, 50]	[-20, 20]	[20, 30]	0.95
N_{e3}	PV bus	1.01	[0, 20]	[0, 20]	[85, 100]	0.95
N_{e4}	PQ bus	[0.969, 1.069]	-	-	[40, 55]	0.90
N_{e5}	PQ bus	[0.97, 1.07]	-	-	[0, 10]	0.90
N_{e6}	PV bus	1.07	0	[-6, 24]	[0, 15]	0.95
N_{e7}	PQ bus	[1.012, 1.112]	-	-	-	-
N_{e8}	PV bus	1.09	0	[-6, 24]	-	-
N_{e9}	PQ bus	[1.006, 1.106]	-	-	[25, 40]	0.95
N_{e10}	PQ bus	[1.001, 1.101]	-	-	[0, 15]	0.95
N_{e11}	PQ bus	[1.007, 1.107]	-	-	[0, 5]	0.95
N_{e12}	PQ bus	[1.005, 1.105]	-	-	[0, 10]	0.95
N_{e13}	PQ bus	[1, 1.1]	-	-	[0, 15]	0.90
N_{e14}	PQ bus	[0.986, 1.086]	-	-	[10, 20]	0.90

TABLE E2
BUS PARAMETERS OF IEEE 14-BUS EPS.

Branch	From	To	Resistance (Ω)	Reactance (Ω)	Susceptance (s)	Transformer ratio	Capacity (MVA)
b_{e1}	N_{e1}	N_{e2}	23.07	70.43	4.43×10^{-5}	-	200
b_{e2}	N_{e1}	N_{e5}	64.31	265.47	4.13×10^{-5}	-	100
b_{e3}	N_{e2}	N_{e3}	55.93	235.63	3.68×10^{-5}	-	100
b_{e4}	N_{e2}	N_{e4}	69.17	209.86	2.86×10^{-5}	-	75
b_{e5}	N_{e2}	N_{e5}	67.78	206.96	2.91×10^{-5}	-	50
b_{e6}	N_{e3}	N_{e4}	79.76	203.57	1.08×10^{-5}	-	50
b_{e7}	N_{e4}	N_{e5}	15.89	50.12	0	-	75
b_{e8}	N_{e4}	N_{e7}	0	248.91	0	0.978	50
b_{e9}	N_{e4}	N_{e9}	0	661.99	0	0.969	25
b_{e10}	N_{e5}	N_{e6}	0	299.97	0	0.932	75
b_{e11}	N_{e6}	N_{e11}	113.05	236.74	0	-	25
b_{e12}	N_{e6}	N_{e12}	146.29	304.48	0	-	25
b_{e13}	N_{e6}	N_{e13}	78.74	155.05	0	-	25
b_{e14}	N_{e7}	N_{e8}	0	209.66	0	-	25
b_{e15}	N_{e7}	N_{e9}	0	130.94	0	-	50
b_{e16}	N_{e9}	N_{e10}	37.86	100.58	0	-	10
b_{e17}	N_{e9}	N_{e14}	151.29	321.82	0	-	25
b_{e18}	N_{e10}	N_{e11}	97.66	228.61	0	-	10
b_{e19}	N_{e12}	N_{e13}	262.95	237.91	0	-	5
b_{e20}	N_{e13}	N_{e14}	203.45	414.23	0	-	10

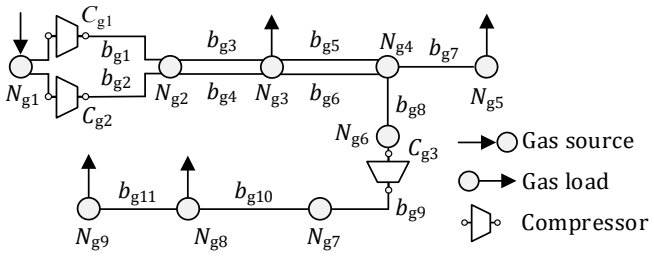

Fig. E2 Structure of southeastern Belgium pipeline system

TABLE E3
NODE PARAMETERS OF SOUTHEASTERN BELGIUM PIPELINE SYSTEM.

Node	Town	Node type	Pressure range (MPa)	Flow range (m^3/s)
N_{g1}	Voeren	Source	[5.5, 6.5]	[-500, 0]
N_{g2}	Berneau	-	[0, 6.5]	-
N_{g3}	Liege	Load	[3, 6.5]	[69, 129]
N_{g4}	Warnand-Dreye	-	[0, 6.5]	-
N_{g5}	Namur	Load	[0, 6.5]	[126, 191]
N_{g6}	Wanze	-	[0, 6.5]	-
N_{g7}	Sinsin	-	[0, 6.3]	-
N_{g8}	Arlon	Load	[0, 6.5]	[0, 30]
N_{g9}	Petange	Load	[2.5, 6.5]	[0, 60]

TABLE E4
PIPE PARAMETERS OF SOUTHEASTERN BELGIUM PIPELINE SYSTEM.

Pipe	From	To	Diameter (10^{-3}m)	Length (km)	Capacity (m^3/s)
b_{g1}	N_{g1}	N_{g2}	890	5	231.5
b_{g2}	N_{g1}	N_{g2}	395.5	5	115.7
b_{g3}	N_{g2}	N_{g3}	890	20	231.5
b_{g4}	N_{g2}	N_{g3}	395.5	20	115.7
b_{g5}	N_{g3}	N_{g4}	890	25	231.5
b_{g6}	N_{g3}	N_{g4}	395.5	25	115.7
b_{g7}	N_{g4}	N_{g5}	890	42	231.5
b_{g8}	N_{g4}	N_{g6}	315.5	10.5	115.7
b_{g9}	N_{g6}	N_{g7}	315.5	26	115.7

b_{g10}	N_{g7}	N_{g8}	315.5	98	115.7
b_{g11}	N_{g8}	N_{g9}	315.5	6	115.7

TABLE E5
COMPRESSOR PARAMETERS OF SOUTHEASTERN BELGIUM PIPELINE SYSTEM.

Compressor	Intake node	Pressure ratio range
C_{g1}	N_{g1}	[1, 1.2]
C_{g2}	N_{g1}	[1, 1.2]
C_{g3}	N_{g6}	[1, 1.2]

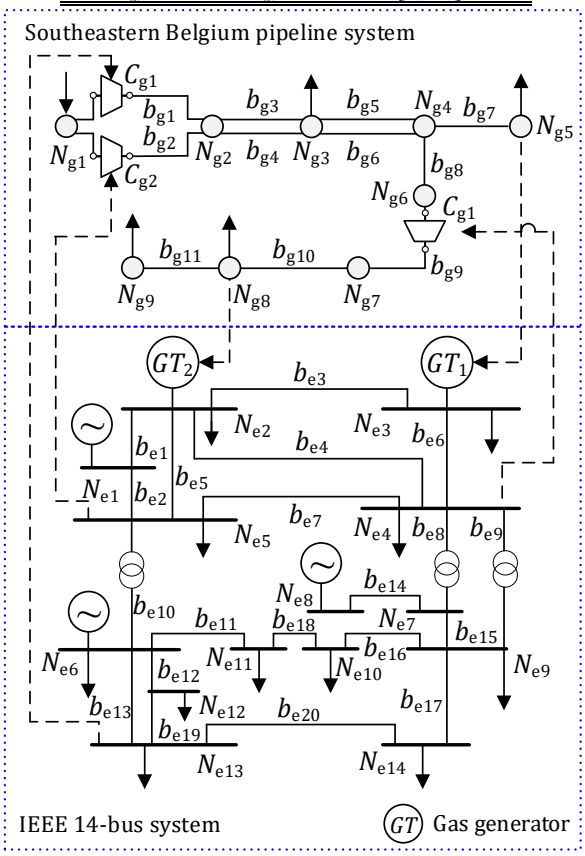

Fig. E3 Structure of 23 node system of IES

TABLE E6
COMPRESSOR PARAMETERS OF 23 NODE SYSTEM OF IES.

Compressor	Intake node	Source for driving	Efficiency	Pressure ratio range
C_{g1}	N_{g1}	N_{e4}	0.8	[1, 1.2]
C_{g2}	N_{g1}	N_{e5}	0.8	[1, 1.2]
C_{g3}	N_{g6}	N_{e13}	0.8	[1, 1.2]

TABLE E7
GAS GENERATOR PARAMETERS OF 23-NODE SYSTEM OF IES.

Genera -tor	Intake node	Heat consumption coefficient a_{GT}	b_{GT}	c_{GT}	d_{GT}	e_{GT}	Output lower limit (MW)
GT_1	N_{g5}	0.01	4	150	15	0.5	0
GT_2	N_{g8}	0.01	4	150	15	0.5	0

F. Comparison of the security region models of IES between the proposed method and existing method

TABLE F1
COMPARISON OF THE SECURITY REGION MODELS OF IES BETWEEN THE PROPOSED METHOD AND EXISTING METHOD.

Security region model based on typical existing method [7]	Energy circuit security region model based on the proposed method

$$\boldsymbol{\Omega}_{\text{IES-SR}}=\left\{\boldsymbol{W}_{\text{s}}\middle|\boldsymbol{h}(\boldsymbol{W}_{\text{s}})=\boldsymbol{0},\boldsymbol{g}(\boldsymbol{W}_{\text{s}})\le\boldsymbol{0}\right\}$$

$$s.t.(1)\begin{cases}P_i=|V_i|\sum_{j=1}^{N}|V_j|\left(G_{ij}\cos\theta_{ij}+B_{ij}\cos\theta_{ij}\right)\\ Q_i=|V_i|\sum_{j=1}^{N}|V_j|\left(G_{ij}\sin\theta_{ij}-B_{ij}\cos\theta_{ij}\right)\\ \boldsymbol{U}_{\text{n}}^{\min}\le\boldsymbol{U}_{\text{n}}\le\boldsymbol{U}_{\text{n}}^{\max}\\ \boldsymbol{P}_{\text{n}}^{\min}\le\boldsymbol{P}_{\text{n}}\le\boldsymbol{P}_{\text{n}}^{\max}\\ \boldsymbol{Q}_{\text{n}}^{\min}\le\boldsymbol{Q}_{\text{n}}\le\boldsymbol{Q}_{\text{n}}^{\max}\\ \boldsymbol{S}_{\text{b}}\le\boldsymbol{S}_{\text{b}}^{\max}\\ \boldsymbol{K}_{\text{e}}^{\min}\le\boldsymbol{K}_{\text{e}}\le\boldsymbol{K}_{\text{e}}^{\max}\end{cases}$$

$$s.t.(2)\begin{cases}-\boldsymbol{A}_{\text{g,L}}^{-1}\boldsymbol{G}_{\text{n}}=\boldsymbol{\eta}_{\text{g}}\boldsymbol{\sigma}_{\text{g}}\sqrt{\left(\boldsymbol{K}_{\text{g}}^{2}\boldsymbol{A}_{\text{g+}}^{\text{T}}\cdot\times\boldsymbol{A}_{\text{g}}^{\text{T}}\right)\boldsymbol{p}_{\text{n}}^{2}}\\ \boldsymbol{p}_{\text{n}}^{\min}\le\boldsymbol{p}_{\text{n}}\le\boldsymbol{p}_{\text{n}}^{\max}\\ \boldsymbol{G}_{\text{n}}^{\min}\le\boldsymbol{G}_{\text{n}}\le\boldsymbol{G}_{\text{n}}^{\max}\\ \boldsymbol{G}_{\text{b}}\le\boldsymbol{G}_{\text{b}}^{\max}\\ \boldsymbol{K}_{\text{g}}^{\min}\le\boldsymbol{K}_{\text{g}}\le\boldsymbol{K}_{\text{g}}^{\max}\end{cases}$$

$$s.t.(3)\begin{cases}\boldsymbol{g}_{\text{m}}=f\left(\boldsymbol{h}_{\text{m}}\right)\\ \boldsymbol{g}_{\text{m}}\subseteq\boldsymbol{F}_{\text{n}},\boldsymbol{h}_{\text{m}}\subseteq\boldsymbol{F}_{\text{n}}\end{cases}$$

$$\boldsymbol{\Omega}_{\text{IES-ECSR}}=\left\{\boldsymbol{W}_{\text{s}}\middle|\boldsymbol{h}(\boldsymbol{W}_{\text{s}})=\boldsymbol{0},\boldsymbol{g}(\boldsymbol{W}_{\text{s}})\le\boldsymbol{0}\right\}$$

$$s.t.(1)\begin{cases}\boldsymbol{Y}_{\text{IES}}\boldsymbol{P}_{\text{n}}=\boldsymbol{F}_{\text{n}}\\ \boldsymbol{P}_{\text{n}}^{\min}\le\boldsymbol{P}_{\text{n}}\le\boldsymbol{P}_{\text{n}}^{\max}\\ \boldsymbol{F}_{\text{n}}^{\min}\le\boldsymbol{F}_{\text{n}}\le\boldsymbol{F}_{\text{n}}^{\max}\\ \boldsymbol{F}_{\text{b}}\le\boldsymbol{F}_{\text{b}}^{\max}\\ \boldsymbol{K}^{\min}\le\boldsymbol{K}_{\text{IES}}\le\boldsymbol{K}^{\max}\end{cases}$$

$$s.t.(2)\begin{cases}\boldsymbol{g}_{\text{m}}=f\left(\boldsymbol{h}_{\text{m}}\right)\\ \boldsymbol{g}_{\text{m}}\subseteq\boldsymbol{F}_{\text{n}},\boldsymbol{h}_{\text{m}}\subseteq\boldsymbol{F}_{\text{n}}\end{cases}$$

G. Explanations of the main formula

TABLE G1
EXPLANATIONS OF THE MAIN FORMULAS

Formula number	Formula	Explanation
(1)	$\boldsymbol{W}=[S_{\text{l,e1}},\ldots,S_{\text{l,e}i},\ldots,S_{\text{l,e}m},G_{\text{l,g1}},\ldots,G_{\text{l,g}j},\ldots,G_{\text{l,g}n}]$	operating point
(2)	$\boldsymbol{W}=[S_{\text{l,e1}},\ldots,S_{\text{l,e}i},\ldots,S_{\text{l,c1}},\ldots,S_{\text{l,c}m},\ldots G_{\text{l,g1}},\ldots,G_{\text{l,g}j},\ldots,G_{\text{l,GT1}},\ldots,G_{\text{l,GT}n},\ldots]$	operating point with compressor and gas generator as coupling units
(3)	$\boldsymbol{\Omega}_{\text{SR}}=\left\{\boldsymbol{W}_{\text{s}}\middle\vert\boldsymbol{h}(\boldsymbol{W}_{\text{s}})=\boldsymbol{0},\ \boldsymbol{g}(\boldsymbol{W}_{\text{s}})\le\boldsymbol{0}\right\}$	security region
(4)	$\boldsymbol{Y}_{\text{e}}\boldsymbol{U}_{\text{n}}=\boldsymbol{I}_{\text{n}}$	electric power network equation
(5)	$r_{\text{g}}=\frac{\lambda_{\text{g}}v_{\text{b}}}{s_{\text{g}}d_{\text{g}}}$	distributed parameter of gas resistance in steady state (characterizing the frictional effect of pipelines on natural gas flow in steady state)
(6)	$L_{\text{g}}=0$	distributed parameter of gas inductance (characterizing the inertia of natural gas flow in steady state)
(7)	$k_{\text{g}}=\frac{2gd_{\text{g}}\sin\theta_{\text{g}}-\lambda_{\text{g}}v_{\text{b}}^{2}}{2RTs_{\text{g}}}$	distributed parameter of controlled gas pressure source (characterizing the influence of pipeline inclination angle and flow velocity changes on pipeline friction in steady state)
(8)	$C_{\text{g}}=0$	distributed parameter of gas capacitance (characterizing the natural gas pipeline storage effect in steady state)

(9) $$Z_{\mathrm{gb}}=2\frac{r_{\mathrm{g}}}{k_{\mathrm{g}}}\cdot\sinh\frac{k_{\mathrm{g}}l_{\mathrm{g}}}{2}\cdot e^{-\frac{k_{\mathrm{g}}l_{\mathrm{g}}}{2}}$$ branch impedance of pipe

(10) $$k_{\mathrm{gb}}=(\cosh\frac{k_{\mathrm{g}}l_{\mathrm{g}}}{2}-\sinh\frac{k_{\mathrm{g}}l_{\mathrm{g}}}{2})e^{-\frac{k_{\mathrm{g}}l_{\mathrm{g}}}{2}}$$ controlled gas pressure source of pipe

(11) $$Y_{\mathrm{gb},10}=0$$ ground admittance of pipe

(12) $$Y_{\mathrm{gb},20}=0$$ ground admittance of pipe

(13) $$\boldsymbol{Y}_{\mathrm{g}}\boldsymbol{p}_{\mathrm{n}}=\boldsymbol{G}_{\mathrm{n}}$$ natural gas network equation

(14) $$\boldsymbol{Y}_{\mathrm{g}}=-\boldsymbol{A}_{\mathrm{g}}\boldsymbol{y}_{\mathrm{gb}}(\boldsymbol{K}_{\mathrm{g}}\boldsymbol{A}_{\mathrm{g}+}^{\mathrm{T}}-\boldsymbol{k}_{\mathrm{gb}}\boldsymbol{A}_{\mathrm{g}+}^{\mathrm{T}}-\boldsymbol{A}_{\mathrm{g}-}^{\mathrm{T}})$$ generalized node admittance matrix of natural gas system

(15) $$\begin{cases}\boldsymbol{\Omega}_{\text{EPS-ECSR}}=\left\{\boldsymbol{W}_{\mathrm{s}}\middle|\boldsymbol{h}(\boldsymbol{W}_{\mathrm{s}})=\boldsymbol{0},\boldsymbol{g}(\boldsymbol{W}_{\mathrm{s}})\le\boldsymbol{0}\right\}\\ s.t.\begin{cases}s.t.(17-1)\ \ \boldsymbol{Y}_{\mathrm{e}}\boldsymbol{U}_{\mathrm{n}}=\boldsymbol{I}_{\mathrm{n}}\\ s.t.(17-2)\ \ \boldsymbol{I}_{\mathrm{n}}^{\min}\le\boldsymbol{I}_{\mathrm{n}}\le\boldsymbol{I}_{\mathrm{n}}^{\max}\\ s.t.(17-3)\ \ \boldsymbol{U}_{\mathrm{n}}^{\min}\le\boldsymbol{U}_{\mathrm{n}}\le\boldsymbol{U}_{\mathrm{n}}^{\max}\\ s.t.(17-4)\ \ \boldsymbol{I}_{\mathrm{b}}\le\boldsymbol{I}_{\mathrm{b}}^{\max}\\ s.t.(17-5)\ \ \boldsymbol{K}_{\mathrm{e}}^{\min}\le\boldsymbol{K}_{\mathrm{e}}\le\boldsymbol{K}_{\mathrm{e}}^{\max}\end{cases}\end{cases}$$ Energy circuit security region of electric power system (EPS-ECSR)

(16) $$\begin{cases}\boldsymbol{\Omega}_{\text{NGS-ECSR}}=\left\{\boldsymbol{W}_{\mathrm{s}}\middle|\boldsymbol{h}(\boldsymbol{W}_{\mathrm{s}})=\boldsymbol{0},\boldsymbol{g}(\boldsymbol{W}_{\mathrm{s}})\le\boldsymbol{0}\right\}\\ s.t.\begin{cases}s.t.(18-1)\ \ \boldsymbol{Y}_{\mathrm{g}}\boldsymbol{p}_{\mathrm{n}}=\boldsymbol{G}_{\mathrm{n}}\\ s.t.(18-2)\ \ \boldsymbol{G}_{\mathrm{n}}^{\min}\le\boldsymbol{G}_{\mathrm{n}}\le\boldsymbol{G}_{\mathrm{n}}^{\max}\\ s.t.(18-3)\ \ \boldsymbol{p}_{\mathrm{n}}^{\min}\le\boldsymbol{p}_{\mathrm{n}}\le\boldsymbol{p}_{\mathrm{n}}^{\max}\\ s.t.(18-4)\ \ -\boldsymbol{A}_{\mathrm{g,L}}^{-1}\boldsymbol{G}_{\mathrm{n}}\le\boldsymbol{G}_{\mathrm{b}}^{\max}\\ s.t.(18-5)\ \ \boldsymbol{K}_{\mathrm{g}}^{\min}\le\boldsymbol{K}_{\mathrm{g}}\le\boldsymbol{K}_{\mathrm{g}}^{\max}\end{cases}\end{cases}$$ Energy circuit security region of natural gas system (EPS-ECSR)

(17) $$\begin{cases}\boldsymbol{\Omega}_{\text{IES-SR}}=\left\{\boldsymbol{W}_{\mathrm{s}}\middle|\boldsymbol{h}(\boldsymbol{W}_{\mathrm{s}})=\boldsymbol{0},\boldsymbol{g}(\boldsymbol{W}_{\mathrm{s}})\le\boldsymbol{0}\right\}\\ s.t.(\mathrm{R1}-1)\text{:}\\ \begin{cases}\boldsymbol{Y}_{\mathrm{IES}}\boldsymbol{P}_{\mathrm{n}}=\boldsymbol{F}_{\mathrm{n}}\\ \boldsymbol{P}_{\mathrm{n}}^{\min}\le\boldsymbol{P}_{\mathrm{n}}\le\boldsymbol{P}_{\mathrm{n}}^{\max}\\ \boldsymbol{F}_{\mathrm{n}}^{\min}\le\boldsymbol{F}_{\mathrm{n}}\le\boldsymbol{F}_{\mathrm{n}}^{\max}\\ \boldsymbol{F}_{\mathrm{b}}\le\boldsymbol{F}_{\mathrm{b}}^{\max}\\ \boldsymbol{K}^{\min}\le\boldsymbol{K}\le\boldsymbol{K}^{\max}\end{cases}\\ s.t.(\mathrm{R1}-2)\text{:}\\ \boldsymbol{g}_{\mathrm{m}}=f\left(\boldsymbol{h}_{\mathrm{m}}\right)\\ \boldsymbol{g}_{\mathrm{m}}\subseteq\boldsymbol{F}_{\mathrm{n}},\boldsymbol{h}_{\mathrm{m}}\subseteq\boldsymbol{F}_{\mathrm{n}}\end{cases}$$ Energy circuit security region of integrated energy system (IES-ECSR)

(18) $$\begin{cases}\boldsymbol{\Omega}_{\text{IES-ECSR}}=\left\{\boldsymbol{W}_{\mathrm{s}}\middle|\boldsymbol{h}(\boldsymbol{W}_{\mathrm{s}})=\boldsymbol{0},\boldsymbol{g}(\boldsymbol{W}_{\mathrm{s}})\le\boldsymbol{0}\right\}\\ s.t.(19-1)\text{:}\\ \begin{cases}\boldsymbol{Y}_{\mathrm{IES}}\boldsymbol{P}_{\mathrm{n}}=\boldsymbol{F}_{\mathrm{n}}\\ \boldsymbol{P}_{\mathrm{n}}^{\min}\le\boldsymbol{P}_{\mathrm{n}}\le\boldsymbol{P}_{\mathrm{n}}^{\max}\\ \boldsymbol{F}_{\mathrm{n}}^{\min}\le\boldsymbol{F}_{\mathrm{n}}\le\boldsymbol{F}_{\mathrm{n}}^{\max}\\ \boldsymbol{F}_{\mathrm{b}}\le\boldsymbol{F}_{\mathrm{b}}^{\max}\\ \boldsymbol{K}^{\min}\le\boldsymbol{K}\le\boldsymbol{K}^{\max}\end{cases}\\ s.t.(19-2)\text{:}\\ \begin{cases}S_{\mathrm{c}}=\dfrac{151.4653\mathrm{p}_0ZTG_c\kappa}{\psi\mathrm{T}_0(\kappa\text{-}1)}(K_{\mathrm{g}}^{\frac{\kappa}{\kappa-1}}-1)\\ G_{\mathrm{GT}}=\dfrac{1}{\mathrm{V}_{\mathrm{GH}}}(a_{\mathrm{GT}}P_{GT}^2+b_{\mathrm{GT}}P_{GT}+c_{\mathrm{GT}}+|\,d_{\mathrm{GT}}\sin(e_{\mathrm{GT}}(P_{\mathrm{GT}}^{\min}-P_{GT}))\,|)\end{cases}\end{cases}$$ IES-ECSR with compressor and gas generator as coupling units